(12)

NOSC

NOSC TR 227

Technical Report 227

(6)

SPECTRAL ESTIMATION OF CONTINUOUS TIME PROCESSES USING POISSON DISTRIBUTED TIME SAMPLES.

(10) C. Mirabile and D. Klamer

(12) 47 p.

(11) 7 April 1978

Research: October 1976 - September 1977

(9) Technical research rept. Oct 76 - Sep 77

NAVAL OCEAN SYSTEMS CENTER
SAN DIEGO, CALIFORNIA 92152

343 159

NAVAL OCEAN SYSTEMS CENTER, SAN DIEGO, CA 92152

AN ACTIVITY OF THE NAVAL MATERIAL COMMAND

RR GAVAZZI, CAPT, USN
Commander

HL BLOOD
Technical Director

ADMINISTRATIVE INFORMATION

The Undersea Surveillance Department was tasked to perform this work under the Independent Research Program.

The work was performed in collaboration with Professor E Masry, University of California, San Diego.

Computer programming support was provided by D Burns.

Released by
DA Hanna, Head
Signal Processing and Display Division

Under authority of
HA Schenck, Head
Undersea Serveillance Department

UNCLASSIFIED
SECURITY CLASSIFICATION OF THIS PAGE *(When Data Entered)*

REPORT DOCUMENTATION PAGE		READ INSTRUCTIONS BEFORE COMPLETING FORM
1. REPORT NUMBER NOSC Technical Report 227 (TR 227)	2. GOVT ACCESSION NO.	3. RECIPIENT'S CATALOG NUMBER
4. TITLE *(and Subtitle)* SPECTRAL ESTIMATION OF CONTINUOUS TIME PROCESSES USING POISSON DISTRIBUTED TIME SAMPLES		5. TYPE OF REPORT & PERIOD COVERED Research: September 1976–October 1977 6. PERFORMING ORG. REPORT NUMBER
7. AUTHOR(s) C. Mirabile and D. Klamer		8. CONTRACT OR GRANT NUMBER(s)
9. PERFORMING ORGANIZATION NAME AND ADDRESS Naval Ocean Systems Center San Diego, California 92152		10. PROGRAM ELEMENT, PROJECT, TASK AREA & WORK UNIT NUMBERS NA
11. CONTROLLING OFFICE NAME AND ADDRESS Naval Ocean Systems Center San Diego, California 92152		12. REPORT DATE 7 April 1978 13. NUMBER OF PAGES 46
14. MONITORING AGENCY NAME & ADDRESS*(if different from Controlling Office)*		15. SECURITY CLASS. *(of this report)* Unclassified 15a. DECLASSIFICATION/DOWNGRADING SCHEDULE

16. DISTRIBUTION STATEMENT *(of this Report)*

Approved for public release; distribution unlimited

17. DISTRIBUTION STATEMENT *(of the abstract entered in Block 20, if different from Report)*

18. SUPPLEMENTARY NOTES

19. KEY WORDS *(Continue on reverse side if necessary and identify by block number)*

Communication–radio systems
Continuous spectra
Density–Estimates–Spectra
Poisson density functions
Probability
Probability density functions
Sampling–Theorems
Signal processing
Spectrum analysis

20. ABSTRACT *(Continue on reverse side if necessary and identify by block number)*

Report compares two discrete time spectral estimation techniques for estimating the spectral density function of a continuous time process – periodic spectral estimation and Poisson spectral estimation. It shows the Poisson to excel when the spectral density is not bandlimited; when the shape of the spectral density is not known a priori; and when the sampling rate is constrained to be below that of Nyquist. The Poisson theory applies to other areas of signal processing. The Poisson technique could be used in applications such as cross spectral estimation, estimation of the coherence function, and antenna array beamforming.

DD FORM 1 JAN 73 1473 EDITION OF 1 NOV 65 IS OBSOLETE
S/N 0102 LF 014 6601

UNCLASSIFIED
SECURITY CLASSIFICATION OF THIS PAGE *(When Data Entered)*

CONTENTS

I.	Introduction	1
II.	Theory	2
III.	Generation of Data	10
IV.	Simulation Results	27
V.	Conclusions	40
References		41
Appendix		43

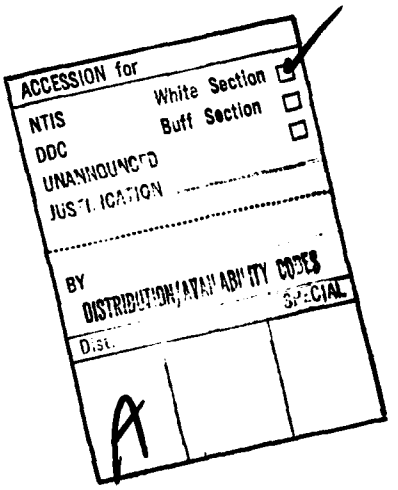

I. INTRODUCTION

The ability to provide good estimates of statistical functions of ocean data is an important area of research within the Naval community. A new approach for estimating one of these statistical functions, the spectral density function, is the focus of work reported here.

In this report we compare two discrete time spectral estimation techniques for estimating the spectral density function of a continuous time process. This comparison consists of theoretical results which give the asymptotic performance of the two spectral estimation schemes along with simulation results for finite sample size estimates. The two spectral estimation schemes considered are periodic spectral estimation and Poisson spectral estimation. In the first case, samples of the continuous time process are taken at discrete instants of time which are equally spaced. The Poisson spectral estimate is based upon samples from the process which are taken at points of time determined by a stationary Poisson point process.

Theoretical asymptotic results for the bias and variance of the Poisson spectral estimate have recently been developed [1, 2] and are very similar to the asymptotic expressions for the bias and variance of the periodic spectral estimate. Since only the asymptotic results are available for the Poisson spectral estimate, the performance of the estimator for a finite number of samples is not known. Hence, an evaluation of the performance of the Poisson spectral estimator for a reasonable number of samples is an important first step in the application of the theoretical results.

II. THEORY

In this section we present the asymptotic behavior of the bias and variance of the periodic and Poisson spectral estimation techniques. The periodic spectral estimator is a consistent estimator of the aliased version of the true spectral density. The Poisson spectral estimator is, however, a consistent estimator of the true spectral density [3, 4]. Similarities between the asymptotic performance of the two estimators are noted. Derivations of these results are presented elsewhere [1].

Throughout this report we let $X = \{X(t), -\infty < t < \infty\}$ be a continuous parameter, zero mean, second order, stationary random process with correlation function $C(t) \in L_1$ and spectral density function $\phi(\lambda)$ given by

$$\phi(\lambda) = \int_{-\infty}^{\infty} C(t)\, e^{-i\lambda t}\, dt/2\pi \ .$$

A spectral window, used to smooth the data used in the spectral estimate, is generated as follows: Let $H(\lambda)$ be a real, even function which satisfies

$$\int_{-\infty}^{\infty} H(\lambda)\, d\lambda = 1$$

$$\int_{-\infty}^{\infty} |H(\lambda)|\, d\lambda < \infty \ .$$

The spectral window, $W_N(\lambda)$, is defined by

$$W_N(\lambda) = M_N\, H\,(M_N \lambda) \ , \tag{II-1}$$

where $M_N > 0$ is such that

$$M_N \to \infty \text{ and } M_N/N \to 0, \text{ as } N \to \infty \ .$$

The corresponding covariance averaging kernel, $w_N(t)$, is given by

$$w_N(t) = h\,(t/M_N) \tag{II-2}$$

where $h(t)$ is the Fourier transform of $H(\lambda)$,

$$h(t) = \int_{-\infty}^{\infty} H(\lambda)\, e^{it\lambda}\, d\lambda \ . \tag{II-3}$$

A. Periodic Spectral Estimation

Let the process $\bar{X}$ be defined as $\bar{X} = \{X(t_n)\}_{n=-\infty}^{\infty}$ where the sample instants $\{t_n\}$ are given by

$$t_n = n/\rho \; ; n = 0, \pm 1, \pm 2, \ldots$$

and $\rho > 0$ is the sampling rate. It then follows [4] that $\bar{X}$ is a wide-sense stationary process with zero mean, covariance sequence

$$c_n = C(n/\rho) \; , n = 0, \pm 1, \ldots$$

and spectral density function

$$s(\lambda) = \rho \sum_{k=-\infty}^{\infty} \phi(\rho\lambda + 2\pi k \rho) \; . \tag{II-4}$$

Note that $s(\lambda)$ has period 2π and is integrable over $[-\pi,\pi]$ with Fourier coefficients

$$c_n = \int_{-\pi}^{\pi} e^{in\lambda} s(\lambda) \, d\lambda \; , n = 0, \pm 1, \ldots \; .$$

Now the spectral density, $s(\lambda)$, of $\bar{X}$ can be estimated by the usual technique of smoothing the periodogram of the discrete-parameter stochastic process $\bar{X}$. The estimate of $s(\lambda)$ based upon the samples $\{X(n/\rho)\}_{n=1}^{N}$ is

$$\hat{s}_N(\lambda) = \int_{-\infty}^{\infty} W_N(\lambda - \mu) \, I_N(\mu) \, d\mu \tag{II-5}$$

where $W_N(\lambda)$ is the spectral window (II-1) and $I_N(\lambda)$ is the periodogram

$$I_N(\lambda) = \frac{1}{2\pi N} \left| \sum_{k=1}^{N} X(k/\rho) \, e^{-ik\lambda} \right|^2 \; . \tag{II-6}$$

We note that aliasing occurs in (II-4) unless $\phi(\lambda)$ is zero for $\lambda \in [-\pi\rho,\pi\rho]$, i.e., $\phi(\lambda)$ cannot be uniquely recovered from $s(\lambda)$ unless $\phi(\lambda) = 0$ outside of $[-\pi\rho,\pi\rho]$. For the special case that $\phi(\lambda)$ is zero outside of $[-\pi\rho,\pi\rho]$, then $\phi(\cdot)$ can be recovered from (II-4) and is given by

$$\phi(\lambda) = \frac{1}{\rho} s(\lambda/\rho) \; . \tag{II-7}$$

In the case in which the process X is bandlimited, say from -W/2 to W/2, then the sampling rate ρ can be chosen large enough so that $\phi(\cdot)$ is zero outside of $[-\pi\rho, \rho\pi]$, i.e. $\pi\rho \geq W/2$ or

$$\rho \geq W/2\pi \ .$$

The quantity $W/2\pi$ (cycles per second) is called the Nyquist rate of sampling and is the minimum rate at which one can sample and still recover the spectral density of the original process X. If X is not bandlimited or the sampling occurs at a rate below the Nyquist rate, then aliasing occurs and $\phi(\lambda)$ cannot be recovered from $s(\lambda)$.

The form of (II-7) motivates the estimate for the case when aliasing occurs. Specifically, define

$$\psi(\lambda) = \frac{1}{\rho} s(\lambda/\rho) = \sum_{k=-\infty}^{\infty} \phi(\lambda + 2\pi k\rho) \ . \tag{II-8}$$

We note that $\psi(\cdot)$ is periodic with period $2\pi\rho$ and integrable over $[-\pi\rho,\pi\rho]$. The estimate of $\psi(\lambda)$ based on the observations $\{X(n/\rho)\}_{n=1}^{N}$ is given by

$$\hat{\psi}_N(\lambda) = \frac{1}{\rho} \hat{s}_N(\lambda/\rho) \tag{II-9}$$

and by (II-5)

$$\hat{\psi}_N(\lambda) = \frac{1}{\rho} \int_{-\infty}^{\infty} W_N\left(\frac{\lambda}{\rho} - \mu\right) I_N(\mu)\, d\mu \ . \tag{II-10}$$

Note that since $\psi_N(\lambda)$, the estimate for $\varphi(\lambda)$, is periodic with period $2\pi\rho$ then at best we can recover $\psi(\lambda)$ from the sampled data. However, as the sampling rate ρ tends to infinity $\psi(\lambda)$ tends to $\phi(\lambda)$.

The form of the estimate (II-10) for $\hat{\psi}_N(\lambda)$ is convenient for obtaining asymptotic properties of the estimator, however, for practical implementation, the following form is used

$$\hat{\psi}_N(\lambda) = \frac{1}{2\pi N\rho} \sum_{j=1}^{N} X^2\left(\frac{j}{\rho}\right) + \frac{1}{\pi N\rho} \sum_{m=1}^{N-1} h\left(\frac{m}{M_N}\right) \cos\left(\frac{\lambda m}{\rho}\right) \sum_{j=1}^{N-m} X\left(\frac{m+j}{\rho}\right) X\left(\frac{j}{\rho}\right) \tag{II-11}$$

where h is defined by (II-3). The above form of $\hat{\psi}_N$ is obtained by substituting (II-6) into (II-10) and making use of (II-1) and (II-2).

We now look at the properties of the estimate $\hat{\psi}_N(\lambda)$. The effects of aliasing will be emphasized.

Theorem 1. Let the covariance function, $C(t)$, of the process X satisfy

(i) $t\,C(t) \in L_1$

(ii) $\sum_{n=1}^{\infty} n\,|C(n/\rho)| < \infty$.

Then the asymptotic mean of the estimate $\hat{\psi}_N(\lambda)$ is given by

$$E\left[\hat{\psi}_N(\lambda)\right] = \int_{-\infty}^{\infty} \left[\frac{1}{\rho} W_N\left(\frac{\lambda-\mu}{\rho}\right)\right] \psi(\mu)\, d\mu + 0\left(\frac{1}{N}\right)$$

as $N \to \infty$ and the $0(1/N)$ term is uniform in λ.

The proof of Theorem 1 is given in [1]. By letting $N \to \infty$ we see that

$$\lim_{N \to \infty} E\left[\hat{\psi}_N(\lambda)\right] = \psi(\lambda)$$

and the estimator $\hat{\psi}_N(\lambda)$ is an asymptotically unbiased estimate of $\psi(\lambda)$. However, recall that we are interested in estimating $\phi(\lambda)$, the spectral density of X, and not $\psi(\lambda)$, the spectral density of $\bar{X}$. From (II-7) and (II-9), the best that we can hope for is an estimate of $\psi(\lambda)$, which contains an aliasing error, $\epsilon(\lambda)$, defined by

$$\epsilon(\lambda) = \psi(\lambda) - \phi(\lambda)$$

$$= \sum_{\substack{k=-\infty \\ k \neq 0}}^{\infty} \phi(\lambda + 2\pi k\rho) \ .$$

Note that the aliasing error is independent of N, the total number of samples used to form the estimate, and therefore cannot be reduced by increasing the sample size.

The following theorem gives the covariance of the estimate $\hat{\psi}_N(\lambda)$ for Gaussian processes.

Theorem 2. Let X be a Gaussian process with covariance function C(t) satisfying

(i) $t\,C(t) \in L_1$

(ii) $\sum_{n=1}^{\infty} n|C(n/\rho)| < \infty$.

Let the spectral window be given by (II-1) and suppose $H(\lambda)$ is bounded and differentiable with bounded derivative. Then asymptotically (as $N \to \infty$)

$$\operatorname{cov}\left[\hat{\psi}_N(\lambda), \hat{\psi}_N(\mu)\right] = 2\pi \frac{M_N}{N}\left[\bar{\delta}_{\lambda,\mu} + \bar{\delta}_{\lambda,-\mu}\right][\phi(\lambda) + \epsilon(\lambda)]^2 \int_{-\infty}^{\infty} H^2(u)du + 0\left(\frac{M_N^2}{N^2}\log\frac{M_N}{N}\right)$$

where $\bar{\delta}_{\lambda,\mu}$ is the $2\pi\rho$-periodic extension of the Kronecker delta function

$$\bar{\delta}_{\lambda,\mu} = \begin{cases} 1 \text{ , if } \lambda - \mu \pmod{2\pi\rho} \\ 0 \text{ , otherwise ,} \end{cases}$$

and the $0(\cdot)$ term is uniform in λ and μ. Moreover,

$$\operatorname{Var}\ \hat{\psi}_N(\lambda) \sim \begin{cases} 2\pi \frac{M_N}{N}[\phi(\lambda) + \epsilon(\lambda)]^2 \int_{-\infty}^{\infty} H^2(u)du \text{ , } \lambda \neq 0 \pmod{\pi\rho} \\ 4\pi \frac{M_N}{N}[\phi(\lambda) + \epsilon(\lambda)]^2 \int_{-\infty}^{\infty} H^2(u)du \text{ , } \lambda = 0 \pmod{\pi\rho} \text{ .} \end{cases}$$

The proof of this theorem follows the proof in [5, Theorem 5.6.2].

The results of Theorem 2 are valid for non-Gaussian processes as well, under additional conditions on the fourth-order cumulant function of the process X [5, 6]. It can now be seen by Theorems 1 and 2 that for Gaussian processes the estimate $\hat{\psi}_N(\lambda)$ converges in the mean-square sense to $\psi(\lambda)$ as $N \to \infty$. However, it does not converge to $\phi(\lambda)$ due to the aliasing error $\epsilon(\lambda)$.

B. Poisson Sampling

The motivation for Poisson sampling is discussed in [1, 2]. Among the sampling schemes which yield consistent estimates of $\phi(\lambda)$ from the observation $\{X(t_k)\}_{n=1}^{N}$, the Poisson sampling scheme is the simplest and the most fundamental [1]. Here we only introduce the estimate and state its bias and covariance for the sake of comparison with the periodic estimate $\hat{\psi}_N(\lambda)$.

Assume that the process X is sampled at instants $\{t_n\}$ given by

$$t_0 = 0 \tag{II-12}$$

$$t_n = t_{n-1} + \alpha_n \, , \quad n = 1, 2, \ldots$$

where the $\{\alpha_n\}$ are independent identically distributed positive random variables with a common exponential distribution $F(x) = 1 - e^{-\beta x}$. It is assumed that the sampling instants $\{t_n\}_{n=0}^{\infty}$ are independent of the process X. Note that β is the average sampling rate and as shown in [2], almost every realization of the point process $\{t_n\}_{n=0}^{\infty}$ has a "density" of points β.

Given the observation $\{X(t_k)\}_{k=1}^{N}$, we consider an estimate $\hat{\phi}_N(\lambda)$ of the spectral density $\phi(\lambda)$ as follows [1]:

$$\hat{\phi}_N(\lambda) = \frac{1}{\pi\beta N} \sum_{n=1}^{N-1} \sum_{k=1}^{N-n} X(t_{k+n}) \, X(t_k) \, h\left(\frac{t_{k+n} - t_k}{M_N}\right) \cos \lambda (t_{k+n} - t_k) \tag{II-13}$$

where $h(t)$ and M_N are as in (II-1) and (II-3). It can be seen that the estimate has an almost identical structure to that of the periodic estimate (II-11). Define the bias of the estimate (II-13) by

$$b\left[\hat{\phi}_N(\lambda)\right] = E\left[\hat{\phi}_N(\lambda)\right] - \phi(\lambda) \, .$$

We then have the following results [1] stated here without proof.

Theorem 1′: Let the covariance function of the process X satisfy $tC(t) \in L_1$. Then, asymptotically as $N \to \infty$,

$$E\left[\hat{\phi}_N(\lambda)\right] = \int_{-\infty}^{\infty} W_N(\lambda - \mu) \, \phi(\mu) \, d\mu + 0\left(\frac{1}{N}\right)$$

where the $0(1/N)$ term is uniform in λ.

Theorem 2′: Let X be Gaussian with covariance function $C(t)$ satisfying $|C(t)| \leq b(t)$ for all t, where $b(t)$ denotes any continuous even nonnegative function on the real line which is nonincreasing over $[0,\infty)$ such that $tb(t) \in L_1$. Let the spectral window be given by (II-1) and suppose $H(\lambda)$ is bounded and differentiable with bounded derivative. Then asymptotically as $N \to \infty$

$$\operatorname{cov}\left[\hat{\phi}_N(\lambda), \hat{\phi}_N(\mu)\right] = 2\pi\beta[\delta_{\lambda,\mu} + \delta_{\lambda,-\mu}]\left[\phi(\lambda) + \frac{C(0)}{2\pi\beta}\right]^2 \int_{-\infty}^{\infty} H^2(u)du$$

$$+ 0\left(\frac{M_N^2}{N^2}\log\frac{M_N}{N}\right) ,$$

where $\delta_{\lambda,\mu}$ is the Kronecker delta function

$$\delta_{\lambda,\mu} = \begin{cases} 1 , \lambda=\mu \\ 0 , \lambda\neq\mu \end{cases} ,$$

and the $0(\cdot)$ term is uniform in λ and μ. Moreover

$$\operatorname{Var}\left[\hat{\phi}_N(\lambda)\right] \sim 2\pi\beta\frac{M_N}{N}\left[\phi(\lambda) + \frac{C(0)}{2\pi\beta}\right]^2 (1 + \delta_{0,\lambda}) \int_{-\infty}^{\infty} H^2(u)du .$$

The results of Theorem 2′ are valid for non-Gaussian processes as well, under additional conditions on the fourth-order cumulant function of the process X [1].

C. Comparison

In order to compare the asymptotic performance of the periodic-estimate (II-11) and the Poisson-estimate (II-13), we assume the two estimates to have the same number of samples N, identical window functions $H(\lambda)$ and identical sampling rates $\rho\equiv\beta$. It is then seen by Theorems 1′ and 2′ that the Poisson-estimate $\hat{\phi}_N(\lambda)$ converges in the mean-square sense, as $N\to\infty$, to the spectral density $\phi(\lambda)$ for any positive value of the average sampling rate β. On the other hand, it is seen by Theorems 1 and 2 that the periodic estimate (II-11) does not converge to $\phi(\lambda)$, as $N\to\infty$, unless $\phi(\lambda) = 0$ for $|\lambda| > \pi\rho$. Comparing now Theorems 1 and 1′, we find that for the periodic-estimate $\hat{\psi}_N(\lambda)$ we have

$$E\left[\hat{\psi}_N(\lambda)\right] = \int_{-\infty}^{\infty}\left[\frac{1}{\rho}W_N\left(\frac{\lambda-\mu}{\rho}\right)\right]\phi(\mu)d\mu + \int_{-\infty}^{\infty}\left[\frac{1}{\rho}W_N\left(\frac{\lambda-\mu}{\rho}\right)\right]\epsilon(\mu)d\mu$$

$$+ 0\left(\frac{1}{N}\right)$$

where the second integral represents the increase in the mean of the estimate due to the aliasing error. On the other hand, for the Poisson estimate $\hat{\phi}_N(\lambda)$ we have

$$E\left[\hat{\phi}_N(\lambda)\right] = \int_{-\infty}^{\infty} W_N(\lambda-\mu)\,\phi(\mu)\,d\mu + 0\left(\frac{1}{N}\right)$$

with no aliasing term and no dependence on the sampling rate β. For the variances of the two estimates, we see by Theorems 2 and 2′ that the variance of the periodic estimate is proportional to $[\phi(\lambda) + \epsilon(\lambda)]^2$ whereas the variance of the Poisson estimate is proportional to $\beta\left[\phi(\lambda) + \frac{C(0)}{2\pi\beta}\right]^2$. It is clear that the aliasing error $\epsilon(\lambda)$ increases the variance of the periodic estimate while for the Poisson estimate the variance is more complex. In fact, as shown in [1], there is an optimal value of β which minimizes, for each fixed λ, the variance and hence the mean-square error of the Poisson estimate, namely

$$\beta_0(\lambda) = C(0)/2\pi\phi(\lambda)\ . \qquad \text{(II-14)}$$

In any case, the relative value of the two variances cannot be determined without specifying $\phi(\lambda)$.

III. GENERATION OF DATA

In this report we consider three spectral density functions which are associated with different second order random processes. Specifically, the spectral density functions considered are

$$\phi(\lambda) = \frac{\alpha/\pi}{\alpha^2 + \lambda^2} \quad , \tag{III-1a}$$

$$\phi(\lambda) = \frac{2a\lambda^2/\pi}{\left(\lambda^2 - \lambda_0^2\right)^2 + 4a^2\lambda^2} \quad , \tag{III-1b}$$

and

$$\phi(\lambda) = \frac{2\,a\lambda^2/\pi}{\left(\lambda^2 - \lambda_0^2\right)^2 + 4a^2\lambda^2} + \frac{2\,a\lambda^2/\pi}{\left(\lambda^2 - \lambda_1^2\right)^2 + 4a^2\lambda^2} \quad . \tag{III-1c}$$

These spectral densities have been chosen because they possess certain characteristics which are found in data obtained from the real world. The first spectral density (III-1a) is a first order Gauss-Markov process. This spectrum is fairly flat and could represent wide-band noise which has a constant spectrum. The second spectral density function (III-1b) could represent a carrier modulated by a narrowband signal. Finally, the last spectral density function (III-1c) represents two closely spaced carriers modulated by narrowband signals.

The remainder of this section describes the generation of data which represent sampled values of the associated random processes. The aliased version of each of the three spectral densities is derived and the dynamic representation of the three spectral densities is obtained. The dynamic representation provides a recursive method of generating the sample values. Finally, the statistics of the random variables which are needed in the dynamic representation are given.

A. First Order Gauss-Markov Spectral Density

The first order Gauss-Markov spectral density function (III-1a) has the simplest structure (Figure 1) of the three spectral densities used in the simulation. It represents a nonbandlimited low pass spectrum and provides a test of the bias of the spectral estimators (II-10) and (II-12). The correlation function R(t), is given by

$$R(t) = e^{-\alpha|t|} \quad .$$

Since the spectral density function is not bandlimited and the mean-square bandwidth also does not exist, we will refer to the half power point (or 3 dB down from the maximum) as

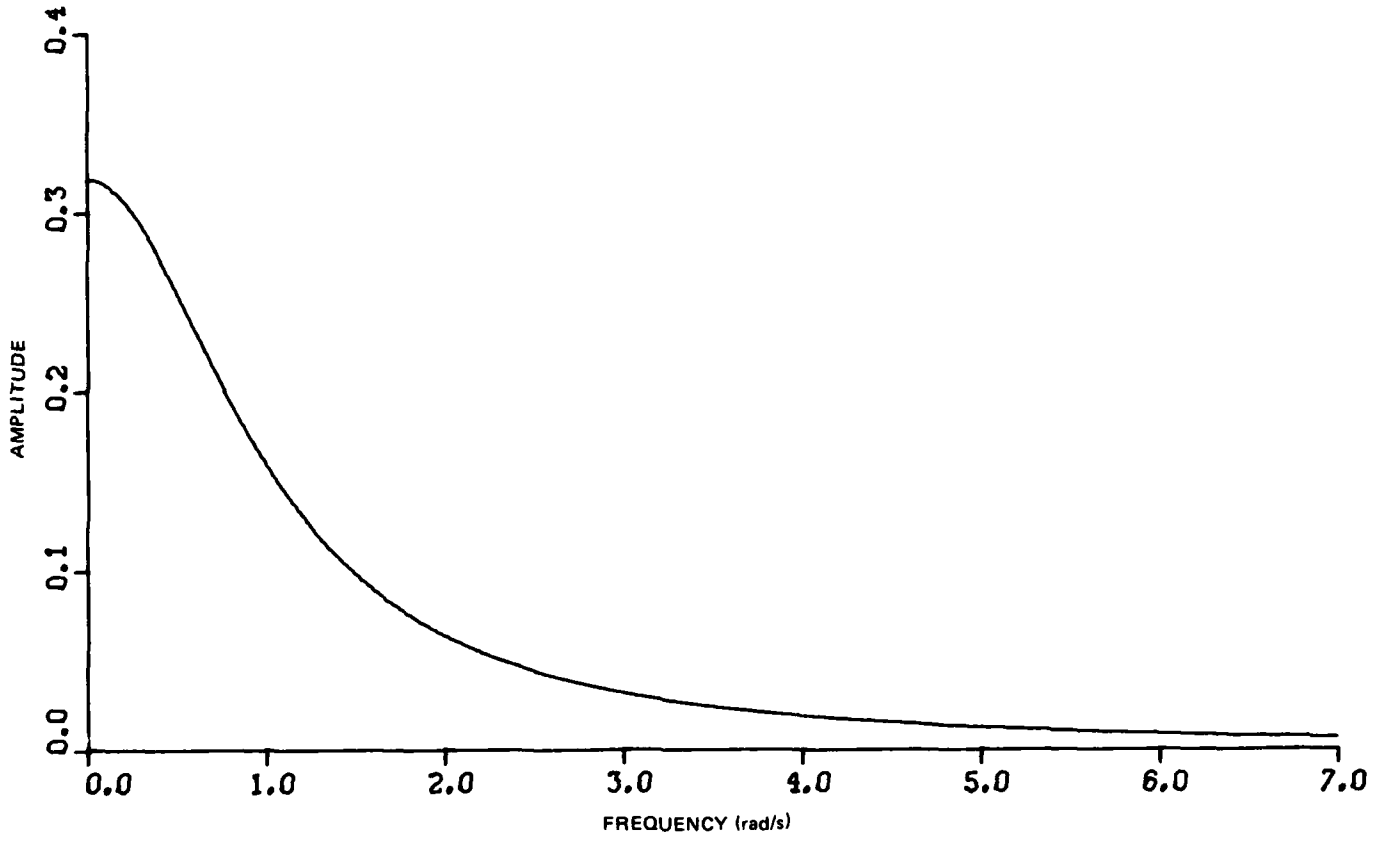

Figure 1. Representation of the "low pass" Gauss-Markov spectral density used in the simulation.

the nominal bandwidth of the process. The nominal bandwidth of (III-1a) is $\lambda = 1.0$ (radians/second).

In this case, the spectral density of the discrete parameter process $\bar{X}$ is an aliased version of $\phi(\lambda)$ and is given by

$$\psi(\lambda) = \sum_{k=-\infty}^{\infty} \phi(\lambda + 2\pi k\rho)$$

$$= \frac{1}{2\pi} \frac{1-q^2}{1+q^2-2q\cos\lambda/\rho}$$

with $q = e^{-\alpha/\rho}$. This follows easily from the Poisson summation formula which gives $s(\lambda)$ as

$$s(\lambda) = \frac{1}{2\pi} \sum_{n=-\infty}^{\infty} R(n/\rho)\, e^{-in\lambda}$$

and $\psi(\lambda)$ can be obtained from $s(\lambda)$ by (II-8).

The Dynamic Representation

Since $\phi(\lambda)$ is a rational spectral density function, the dynamic representation of the associated process can be obtained via the procedure outlined in the appendix. We have

$$\phi(\lambda) = \frac{\alpha}{\pi}\left|\frac{1}{i\lambda+\alpha}\right|^2$$

and by (A-2)

$$X'(t) + FX(t) = Gu(t)$$

where $u(t)$ is a Gaussian white noise process with correlation function $\delta(t)/2\alpha$, $F = -\alpha$, and $G = \sqrt{2\alpha}$. Then by (A-4)

$$X(t) = \Phi(t-\tau)\, X(\tau) + \int_{\tau}^{t} \Phi(t-\nu)\, G\, u(\nu)d\nu \qquad \text{(III-2)}$$

where $\Phi(t-\tau)$ is given by (A-5).

Therefore, a recursive representation is obtained for the process by replacing t with t_{k+1} and τ by t_k in equation (III-2). This yields

$$X(t_{k+1}) = e^{-\alpha(t_{k+1}-t_k)} X(t_k) + G \int_{t_k}^{t_{k+1}} e^{-\alpha(t_{k+1}-\nu)} u(\nu)\, d\nu$$

$$= e^{-\alpha(t_{k+1}-t_k)} X(t_k) + G\,\epsilon_k \qquad \text{(III-3)}$$

with

$$\epsilon_k = \int_{t_k}^{t_{k+1}} e^{-\alpha(t_{k+1} - \nu)} u(\nu)\, d\nu \ .$$

In order to simulate the X process the $\{t_k\}$ must be known and the ϵ_k must be obtained. Let $X(t_o) = X(0) \equiv 0$. The ϵ_k are zero mean Gaussian random variables since they are obtained by a linear operation (integration) on Gaussian random variables u(t). Now only the variance of ϵ_k has to be obtained in order to completely specify the behavior of the X process at the instants $\{t_k\}$.

The variance of ϵ_k is computed as follows

$$E\,\epsilon_k^2 = E \int_{t_k}^{t_{k+1}} \int_{t_k}^{t_{k+1}} e^{-\alpha(t_{k+1} - \nu)} e^{-\alpha(t_{t+1} - \eta)} u(\nu)u(\eta)d\nu d\eta$$

$$= \int_{t_k}^{t_{k+1}} \int_{t_k}^{t_{k+1}} e^{-\alpha(t_{k+1} - \nu)} e^{-\alpha(t_{k+1} - \eta)} \delta(\nu - \eta)d\nu d\eta$$

$$= \int_{t_k}^{t_{k+1}} e^{-2\alpha(t_{k+1} - \nu)} d\nu$$

$$= \frac{1}{2\alpha}\left[1 - e^{-2\alpha(t_{k+1} - t_k)}\right] .$$

The variance of $\eta_k = G\,\epsilon_k$ is

$$E\eta_k^2 = G^2 \cdot E\epsilon_k^2 = R(0)\left[1 - e^{-2\alpha(t_{k+1} - t_k)}\right] . \qquad \text{(III-4)}$$

Also, it can be shown that the ϵ_k are independent random variables. This follows from the definition of ϵ_k in terms of the white Gaussian noise which makes the ϵ_k uncorrelated, and since the ϵ_k are Gaussian it follows that they are, in fact, independent.

Poisson Sampling Model

The following model describes the method used to generate the sampling points and the values of the process at the sampling points. Let the sampling instants $\{t_k\}$ be generated by a Poisson point process (II-12).

Then the dynamic representation is

$$X(0) = 0$$

$$X(t_{k+1}) = e^{-\alpha(t_{k+1} - t_k)} X(t_k) + \eta_k$$

where the t_k are given by (II-12) and η_k is a sequence of independent zero mean Gaussian random variables with variance (equation (III-4))

$$\sigma^2_{\eta_k} = \left[1 - e^{-2(t_{k+1} - t_k)}\right] .$$

Note that the variance will change for each k.

Periodic Sampling Model

In the model for the periodic sampling case the $\{t_k\}$ are determined by

$$t_k = kh, \; k = 0, 1, 2, \ldots \qquad \text{(III-5)}$$

where h is the time between samples. The sampling rate, ρ, is given by

$$\rho = 1/h .$$

Let $X_k = X(kh)$. Then the dynamic representation simplifies to

$$X_o = 0$$

$$X_{k+1} = e^{-\alpha h} X_k + \theta_k$$

where the $\{\theta_k\}$ are independent identically distributed zero mean Gaussian random variables with variance

$$\sigma^2_{\theta_k} = [1 - e^{-2/\rho}] .$$

Note that the variance of θ_k does not depend upon k.

B. The Narrowband Spectral Density

The spectral density used to represent the process X for the narrowband case is given by

$$\phi(\lambda) = \frac{2a}{\pi} \frac{\lambda^2}{\left(\lambda^2 - \lambda_o^2\right)^2 + 4a^2 \lambda^2} \qquad \text{(III-6)}$$

where $2a/\pi$ is a normalization constant such that the correlation function evaluated at 0 is equal to 1, i.e., $R(0) = 1$. A representative form of the spectral density given by equation (III-6) is shown in Figure 2. The correlation function is given by

$$R(t) = \int_{-\infty}^{\infty} \phi(\lambda)\, e^{it\lambda}\, d\lambda$$

$$= e^{-at}\left(\cos w_o t - \frac{a}{w_o} \sin w_o t\right), \; t > 0 \qquad \text{(III-7)}$$

where

$$w_o^2 = \lambda_o^2 - a^2 \; .$$

The maximum of the spectral density occurs at $\lambda = \lambda_o$ and is

$$\phi(\lambda_o) = 1/2\pi a \; . \qquad \text{(III-8)}$$

The half-power point, λ_h, is obtained by solving

$$\phi(\lambda_h) = \phi(\lambda_o)/2$$

for λ_h which yields

$$\lambda_h = \sqrt{2a^2 + \lambda_o^2 + 2a\sqrt{a^2 + \lambda_o^2}} \; . \qquad \text{(III-9)}$$

By adjusting λ_o and λ_h, the "bandwidth" of the narrowband stochastic signal can be made to provide an appropriately narrow peak to the spectral density.

The aliased version $s(\lambda)$ of (III-6) is derived as follows. Let $r(n)$ be the correlation function of the discrete random process $\bar{X}$. Then $r(n) = R(n/\rho)$ where $R(\cdot)$ is the correlation function of the continuous time random process. Therefore, $s(\lambda)$ is given by the Poisson summation formula as

$$s(\lambda) = \frac{1}{2\pi} \sum_{n=-\infty}^{\infty} R(n/\rho)\, e^{-in\lambda} \; . \qquad \text{(III-10)}$$

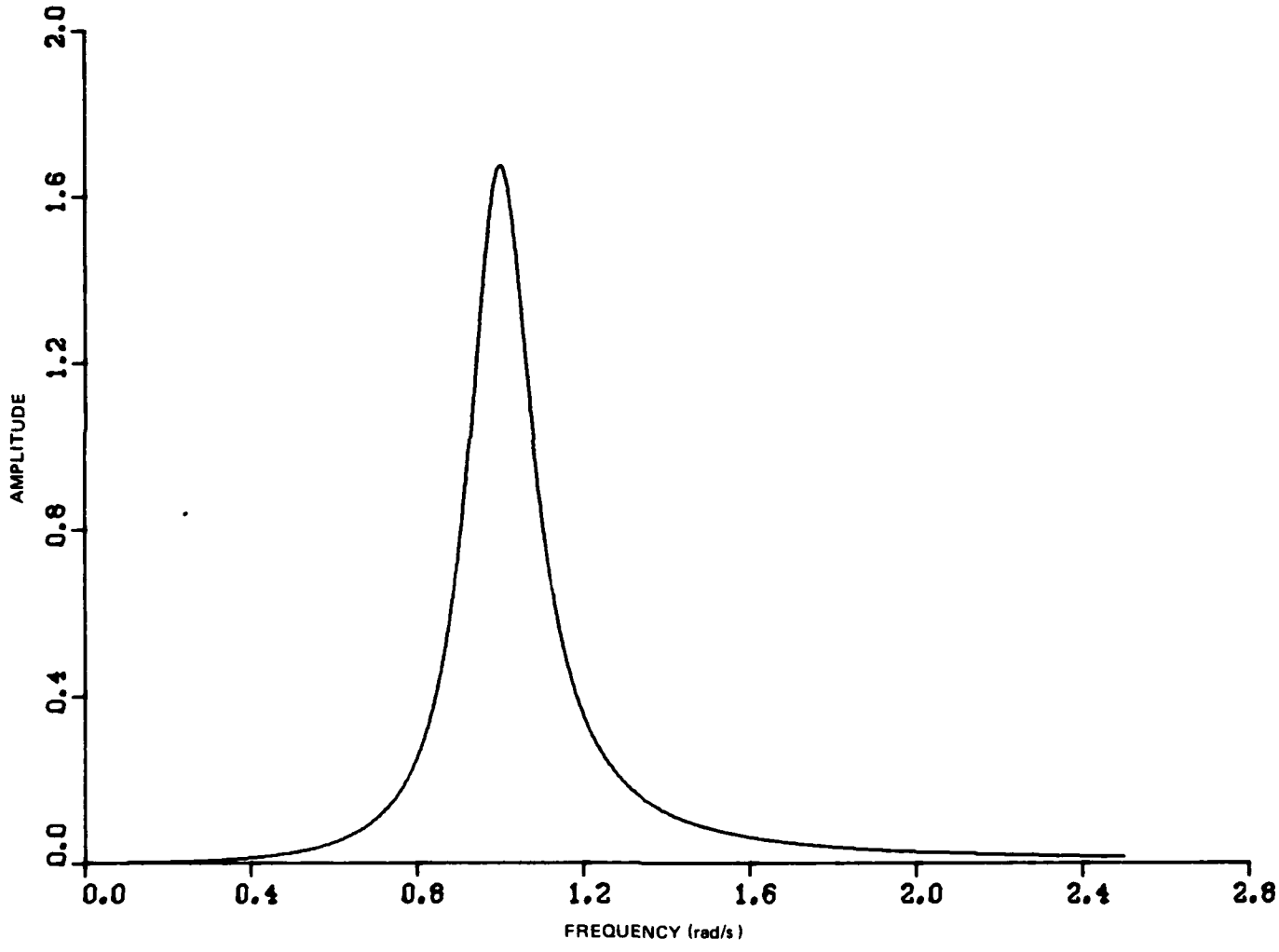

Figure 2. "Narrowband" spectral density used as the second case studied for the simulation.

Since $R(\cdot)$ is an even function, $s(\cdot)$ may be rewritten as

$$s(\lambda) = \frac{1}{2\pi}\left\{R(0) + \sum_{n=1}^{\infty} R(n/\rho)\, e^{-in\lambda} + \sum_{n=1}^{\infty} R(n/\rho)\, e^{in\lambda}\right\}$$

$$= \frac{1}{2\pi}\left\{R(0) + 2\,\mathrm{Re}\sum_{n=1}^{\infty} R(n/\rho)\, e^{-in\lambda}\right\} .$$

From (III-7) the correlation function can be written as

$$R(\tau) = \frac{w_o+ia}{2w_o} e^{i\tau(w_o+ia)} + \frac{w_o-ia}{2w_o} e^{i\tau(-w_o+ia)} .$$

Now

$$\sum_{n=1}^{\infty} R(n/\rho)\, e^{-in\lambda} = \frac{w_o+ia}{2w_o} \sum_{n=1}^{\infty} e^{in[(w_o+ia)/\rho-\lambda]}$$

$$+ \frac{w_o-ia}{2w_o} \sum_{n=1}^{\infty} e^{in[(-w_o+ia)/\rho-\lambda]}$$

$$= \frac{w_o+ia}{2w_o} \frac{e^{(iw_o-a)/\rho-i\lambda}}{1-e^{(iw_o-a)/\rho-i\lambda}} + \frac{w_o-ia}{2w_o} \frac{e^{(iw_o-a)/\rho-i\lambda}}{1-e^{(-iw_o-a)/\rho-i\lambda}}$$

$$= \frac{e^{-a/\rho}}{2w_o}\left\{(w_o+ia)\frac{\cos B^- + i\sin B^- - e^{-a/\rho}}{1+e^{-2a/\rho}-2e^{-a/\rho}\cos B^-}\right.$$

$$\left. + (w_o-ia)\frac{\cos B^+ - i\sin B^+ - e^{-a/\rho}}{1+e^{-2a/\rho}-2e^{-a/\rho}\cos B^+}\right\}$$

where

$$B^+ = w_o/\rho + \lambda \quad \text{and} \quad B^- = w_o/\rho - \lambda .$$

Therefore,

$$2\,\mathrm{Re}\sum_{n=1}^{\infty} R(n/\rho)\, e^{-in\lambda}$$

$$= e^{-a/\rho}\left\{\frac{\cos B^- - e^{-a/\rho} - \frac{a}{w_o}\sin B^-}{1+e^{-2a/\rho}-2e^{-a/\rho}\cos B^-} + \frac{\cos B^+ - e^{-a/\rho} - \frac{a}{w_o}\sin B^+}{1+e^{-2a/\rho}-2e^{-a/\rho}\cos B^+}\right\}$$

Hence, the aliased spectral density is

$$s(\lambda) = \frac{1}{2\pi}\left\{1 + \frac{e^{-a/\rho}\left(\cos B^- - e^{-a/\rho} - \frac{a}{w_o}\sin B^-\right)}{1 + e^{-2a/\rho} - 2e^{-a/\rho}\cos B^-} + \frac{e^{-a/\rho}\left(\cos B^+ - e^{-a/\rho} - \frac{a}{w_o}\sin B^+\right)}{1 + e^{-2a/\rho} - 2e^{-a/\rho}\cos B^+}\right\} .$$

By (II-8) the scaled version of the aliased spectral density in which we are interested is given by

$$\psi(\lambda) = \frac{1}{2\pi\rho}\frac{1-q^4+2\left[(q^3-q)\cos\frac{w_0}{\rho} - \frac{a}{w_0}(q^3+q)\sin\frac{w_0}{\rho}\right]\cos\frac{\lambda}{\rho} + 2\frac{a}{w_0}q^2\sin\frac{2w_0}{\rho}}{(1+q^2)^2 - 4(q^3-q)\cos\frac{w_0}{\rho}\cos\frac{\lambda}{\rho} + 2q^2\left(\cos\frac{2w_0}{\rho} + \cos\frac{2\lambda}{\rho}\right)} \qquad \text{(III-11)}$$

where $q = e^{-a/\rho}$.

The Dynamic Representation

From (A-1) we have

$$\phi(\lambda) = \frac{2a}{\pi}\left|\frac{i\lambda}{(i\lambda)^2 + 2a(i\lambda) + \lambda_o^2}\right|^2 \qquad \text{(III-12)}$$

and by (A-2) the dynamic representation for the process X is

$$X''(t) + 2a\,X'(t) + \lambda_o^2\,X(t) = u'(t) .$$

Using (A-3) the F and G matrix becomes

$$F = \begin{bmatrix} -2a & 1 \\ -\lambda_o^2 & 0 \end{bmatrix} , \qquad \text{(III-13a)}$$

$$G = \begin{bmatrix} 1 \\ 0 \end{bmatrix} . \qquad \text{(III-13b)}$$

In addition X(t) has the representation (A-4)

$$X(t) = \Phi(t,t_o)\,X(t_o) + \int_{t_o}^{t} \Phi(t,\tau)\,G(\tau)\,U(\tau)\,d\tau$$

where Φ, the state transition matrix, satisfies the (deterministic) differential equation

$$\frac{d\Phi(t,t_o)}{dt} = F\,\Phi(t) \ . \qquad \text{(III-14)}$$

Taking the Laplace transform of equation (III-14) and using the fact that $\phi(t,t) = I$ yields

$$s\hat{\Phi}(s) - I = F\,\hat{\Phi}(s) \qquad \text{(III-15)}$$

where $\hat{\Phi}(s)$ is the Laplace transform of

$$\Phi(t) = \begin{bmatrix} \phi_{11}(t) & \phi_{12}(t) \\ \phi_{21}(t) & \phi_{22}(t) \end{bmatrix} .$$

Solving (III-15) for $\hat{\Phi}(s)$ and using (III-13a) gives

$$\hat{\Phi}(s) = (sI-F)^{-1}$$

$$= \frac{1}{s^2 + 2as + \lambda_o^2} \begin{bmatrix} s & 1 \\ -\lambda_o^2 & s+2a \end{bmatrix} . \qquad \text{(III-16)}$$

Taking the inverse Laplace transform of (III-16), the state transition matrix becomes

$$\phi_{11}(t) = e^{-at}\left(\cos w_o\, t - \frac{a}{w_o}\sin w_o\, t\right) \qquad \text{(III-17a)}$$

$$\phi_{12}(t) = \frac{1}{w_o}\, e^{-at} \sin w_o\, t \qquad \text{(III-17b)}$$

$$\phi_{21}(t) = -\frac{\lambda^2}{w_o}\, e^{-at} \sin w_o\, t \qquad \text{(III-17c)}$$

$$\phi_{22}(t) = e^{-at}\left(\cos w_o\, t + \frac{a}{w_o}\sin w_o\, t\right) . \qquad \text{(III-17d)}$$

The recursive dynamic representation with $t_o = 0$ is then

$$X(t_{k+1}) = X_1(t_{k+1}) = \phi_{11}(t_{k+1}-t_k)\,X(t_k) + \phi_{12}(t_{k+1}-t_k)\,X_2(t_k)$$

$$+ \int_{t_k}^{t_{k+1}} \phi_{11}(t_{k+1}-\tau)\,u(\tau)\,d\tau \qquad \text{(III-18a)}$$

and

$$X_2(t_{k+1}) = \phi_{21}(t_{k+1}-t_k)\,X(t_k) + \phi_{22}(t_{k+1}-t_k)\,X_2(t_k)$$

$$+ \int_{t_k}^{t_{k+1}} \phi_{21}(t_{k+1}-\tau)\,u(\tau)\,d\tau \qquad \text{(III-18b)}$$

Define the random variables θ_k and η_k as

$$\theta_k = \int_{t_k}^{t_{k+1}} \phi_{11}(t_{k+1}-\tau)\, u(\tau)\, d\tau \ , \qquad k = 0, 1, 2, \ldots$$

$$\eta_k = \int_{t_k}^{t_{k+1}} \phi_{21}(t_{k+1}-\tau)\, u(\tau) d\tau \ , \qquad k = 0, 1, 2, \ldots \ .$$

and assume the initial values of X and X_2 are zero, i.e.,

$$X(0) = X_2(0) = 0 \ .$$

Since $u(\tau)$ is a zero mean white Gaussian noise the random variables θ_k and η_k are also Gaussian random variables with 0 means. The sequences $\{\theta_k\}_{k=1}^{\infty}$ and $\{\eta_k\}_{k=1}^{\infty}$ are each a sequence of independent random variables since each θ_k (and η_k) is generated by white Gaussian noise over distinct time intervals. However, θ_k is correlated with η_k since the time interval of noise which generates each random variable is the same. Note that θ_k and η_n for $k \neq n$ are independent by the same reasoning as above.

In order to completely describe θ_k and η_k an expression for their variances must be computed. The spectral density for the white Gaussian noise, u(t), is constant and equal to

$$\phi_u(\lambda) = 2a/\pi$$

and the correlation function of u(t) is given by

$$R_u(t) = 2\pi \cdot 2a\, \delta(t)/\pi = 4a\, \delta(t) \ .$$

The variance of θ_k is

$$\sigma_{\theta_k}^2 = E|\theta_k|^2 = 4a \int_{t_k}^{t_{k+1}} \phi_{11}^2(t_{k+1}-\tau)dt$$

$$= 4a \int_{0}^{\Delta_k} \phi_{11}^2(\tau)dt$$

$$= 1 + e^{-2a\Delta_k} \left(a w_o \sin 2w_o\Delta_k + a^2 \cos 2w_o\Delta_k - \lambda_o^2\right)/w_o^2 \qquad \text{(III-19)}$$

where

$$\Delta_k = t_{k+1} - t_k$$

$$w_o^2 = \lambda_o^2 - a^2 \ .$$

Similarly, the variance of η_k is

$$\sigma^2_{\eta_k} = \lambda_o^2 - \lambda_o^2 e^{-2a\Delta_k} \left(aw_o \sin 2 w_o \Delta_k - a^2 \cos 2 w_o \Delta_k + \lambda_o^2\right)/w_o^2 \qquad \text{(III-20)}$$

The cross correlation of θ_k and η_k is given by

$$r_k = E\,\theta_k \eta_k = 4a \int_0^{\Delta_k} \phi_{11}(t)\,\phi_{21}(t)\,dt$$

$$= a\lambda_0^2 e^{-2a\Delta_k} (\cos 2 w_o \Delta_k - 1)/w_o^2 ,$$

and the correlation coefficient is

$$\rho_k = r_k/\sigma_{\theta_k}\,\sigma_{\eta_k} \quad . \qquad \text{(III-21)}$$

We now have the dynamic representation for the narrowband process X(t), with initial conditions $t_o = 0$, $X(0) = X_2(0) = 0$ given recursively by

$$X(t_{k+1}) = \phi_{11}(\Delta_k)\,X(t_k) + \phi_{12}(\Delta_k)\,X_2(t_k) + \theta_k \qquad \text{(III-22a)}$$

$$X_2(t_{k+1}) = \phi_{21}(\Delta_k)\,X(t_k) + \phi_{22}(\Delta_k)\,X_2(t_k) + \eta_k \qquad \text{(III-22b)}$$

where $\Delta_k = t_{k+1} - t_k$, the $\phi_{ij}(\cdot)$ are given by equations (III-17a) -- (III-17d), and the θ_k and η_k are correlated zero mean Gaussian random variables with variances $\sigma_{\theta_k}{}^2$ and $\sigma_{\eta_k}{}^2$ given by (III-19) and (III-20) with correlation coefficient ρ_k (III-21).

The generation of the narrowband data is begun by transforming two sequences of independent zero mean Gaussian random variables into two sequences of correlated random variables with a specified cross correlation. This transformation will provide the proper method of generating sequences of the random variables η_k and θ_k. Given two sequences of zero mean, unit variance Gaussian random variables $\{X_k\}$ and $\{Y_k\}$ we will obtain the transformation which will yield two sequences of Gaussian random variables $\{\theta_k\}$ and $\{\eta_k\}$ with variances $\left\{\sigma^2_{\theta_k}\right\}$, $\left\{\sigma^2_{\eta_k}\right\}$, respectively, and correlation coefficients $\{\rho_k\}$.

For simplicity of analysis the time subscript, k, will be omitted. Let

$$\begin{bmatrix} W \\ Z \end{bmatrix} = \begin{bmatrix} \cos\alpha & -\sin\alpha \\ \sin\alpha & \cos\alpha \end{bmatrix} \begin{bmatrix} \theta \\ \eta \end{bmatrix} \qquad \text{(III-23)}$$

where θ, η are the desired Gaussian random variables. Note that

$$\begin{bmatrix} \theta \\ \eta \end{bmatrix} = \begin{bmatrix} \cos\alpha & \sin\alpha \\ -\sin\alpha & \cos\alpha \end{bmatrix} \begin{bmatrix} W \\ Z \end{bmatrix} . \qquad \text{(III-24)}$$

We will find the appropriate $\alpha = \alpha(\sigma_1, \sigma_2, \rho)$ such that W and Z are independent. Also, we find the variances, σ^2_W and σ^2_Z, of W and Z.

Since W and Z are Gaussian random variables, then orthogonality and independence are equivalent. Therefore, from (III-23)

$$0 = EWZ = \frac{1}{2}\left(\sigma_\eta^2 - \sigma_\theta^2\right) \sin 2\alpha + \rho\sigma_\theta\sigma_\eta \cos 2\alpha$$

and solving for α yields

$$\alpha_k = \frac{1}{2}\tan^{-1}\left[2\rho\sigma_{\theta_k}\sigma_{\eta_k}\left(\sigma_{\eta_k}^2 - \sigma_{\theta_k}^2\right)\right] . \tag{III-25}$$

Now, for the variances of W and Z, we compute

$$EZ^2 = \frac{\sigma_\theta^2+\sigma_\eta^2}{2} + \frac{\sigma_\theta^2-\sigma_\eta^2}{2}\cos 2\alpha - \sigma_\theta\sigma_\eta\rho \sin 2\alpha .$$

Restoring the subscripts and using (III-25) for tan 2α yields

$$\sigma_{Z_k}^2 = \frac{\sigma_{\theta_k}^2 + \sigma_{n_k}^2}{2} - \frac{1}{2}\sqrt{\left(\sigma_{\eta_k}^2 - \sigma_{\theta_k}^2\right)^2 + 4\rho_k^2\sigma_{\theta_k}^2\sigma_{\eta_k}^2} . \tag{III-26}$$

Similarly,

$$\sigma_{W_k}^2 = \frac{\sigma_{\theta_k}^2 + \sigma_{\eta_k}^2}{2} + \frac{1}{2}\sqrt{\left(\sigma_{\eta_k}^2 - \sigma_{\theta_k}^2\right)^2 + 4\rho_k^2\sigma_{\theta_k}^2\sigma_{\eta_k}^2} . \tag{III-27}$$

It can now be seen that the observations $\{X(t_k)\}_{k=1}^N$ can be generated recursively by Monte Carlo simulation as follows:

(i) Obtain from a zero mean, unit variance Gaussian random number generator two sequences of numbers $\{X_k\}_{k=1}^N$ and $\{Y_k\}_{k=1}^N$. Also, obtain a realization of the sampling points $\{t_k\}_{k=1}^N$. For the data used in the periodic spectral estimate the set $\{t_k\}$ is obtained by (III-5) and for the Poisson case by (II-12).

(ii) Compute Var $[\theta_k]$, Var $[\eta_k]$, and ρ_k from (III-19), (III-20) and (III-21) respectively.

(iii) Compute Var $[W_k]$, Var $[Z_k]$, and α_k from (III-27), (III-26) and (III-25).

(iv) Set $W_k = \{\text{Var}[W_k]\}^{1/2} X_k$ and $Z_k = \{\text{Var}[Z_k]\}^{1/2} Y_k$

(v) Compute θ_k and η_k.

(vi) Finally, compute $X_2(t_{k+1})$ from (III-22b) and then the observation $X(t_{k+1})$ by (III-22a).

C. TWO CLOSELY SPACED NARROWBAND SIGNALS

A spectral density resembling two closely spaced narrowband stochastic signals is the final spectral density case investigated (see Figure 3). This data set demonstrates the ability of the Poisson spectral estimation algorithm to resolve two narrowband signals closely spaced in frequency. The spectral density is of the form,

$$\phi(\lambda) = \frac{2\,a\lambda^2/\pi}{\left(\lambda^2 - \lambda_0{}^2\right)^2 + 4\,a^2\lambda^2} + \frac{2\,a\lambda^2/\pi}{\left(\lambda^2 - \lambda_1{}^2\right)^2 + 4\,a^2\lambda^2} \qquad \text{(III-28)}$$

where λ_0 and λ_1 are the center frequencies of each narrowband signal and a is as previously defined.

In this case we assume that X_0 and X_1 are two zero mean independent random processes with correlation functions

$$R_{x_i}(\tau) = e^{-a\tau}\left(\cos w_i\,\tau - \frac{a}{w_i}\sin w_i\,\tau\right), \quad i = 0,1$$

where

$$w_i^2 = \lambda_i^2 - a^2 \qquad i = 0,1$$

and corresponding spectral densities

$$\phi_j(\lambda) = \int_{-\infty}^{\infty} e^{i\lambda\tau} R_{x_j}(\tau)\,d\tau = \frac{2\,a\,\lambda^2/\pi}{\left(\lambda^2 - \lambda_j^2\right)^2 + 4\,a^2\lambda^2} \quad j = 0,1$$

Define the process X(t) as

$$X(t) = X_0(t) + X_1(t)\,.$$

We then have by using the assumption that $X_0(t)$ and $X_1(t)$ are independent that

$$R_X(\tau) = E\,X_0(t+\tau)\,X_0(t) + E\,X_1(t+\tau)\,X_1(t) = R_{x_0}(\tau) + R_{x_1}(\tau)$$

and therefore

$$\phi(\lambda) = \phi_0(\lambda) + \phi_1(\lambda)$$

$$= \frac{2a\,\lambda^2/\pi}{\left(\lambda^2 - \lambda_0{}^2\right)^2 + 4\,a^2\lambda^2} + \frac{2a\,\lambda^2/\pi}{\left(\lambda^2 - \lambda_1{}^2\right)^2 + 4\,a^2\lambda^2}\,.$$

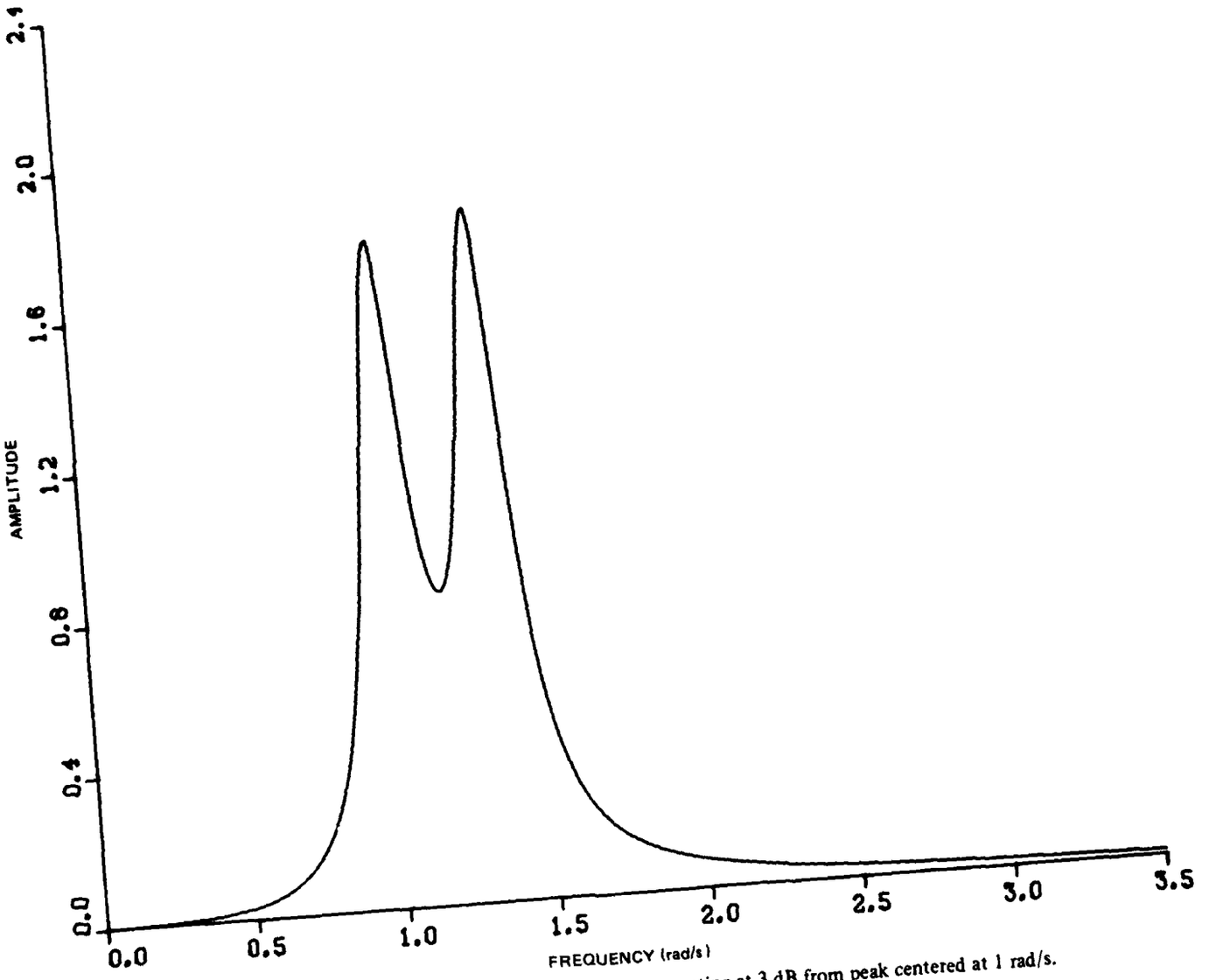

Figure 3. Two closely spaced "narrowband" signals intersecting at 3 dB from peak centered at 1 rad/s. Used as final data set for the simulation.

The aliased version of $\phi(\lambda)$ is

$$\psi(\lambda) = \psi_0(\lambda) + \psi_1(\lambda)$$

where $\psi_0(\lambda)$ and $\psi_1(\lambda)$ are as in (III-11) .

$$\psi_i(\lambda) = \frac{1}{2\pi\rho} \; \frac{1-q^4+2\left[(q^3-q)\cos\frac{w_i}{\rho} - \frac{a}{w_i}(q^3+q)\sin\frac{w_i}{\rho}\right]\cos\frac{\lambda}{\rho} + 2\,w_i\,q^2\sin\frac{2w_i}{\rho}}{(1+q^2)^2 - 4(q^3-q)\cos\frac{w_i}{\rho}\cos\frac{\lambda}{\rho} + 2q^2\left(\cos\frac{2w}{\rho}i + \cos\frac{2\lambda}{\rho}\right)}$$

where $q = e^{-a/\rho}$, i=0,1

All other parameters are as previously defined.

The Dynamic Representation

Since the spectral density $\phi(\lambda)$ is of the form

$$\phi(\lambda) = \left|\frac{P_0(i\lambda)}{Q_0(i\lambda)}\right|^2 + \left|\frac{P_1(i\lambda)}{Q_1(i\lambda)}\right|^2$$

then the dynamic representation of the process X(t) is simply the addition of the dynamic representations for $X_0(t)$ and $X_1(t)$. These dynamic representations are derived in exactly the same manner as for the narrowband case considered in the last section.

The process X(t) for this case is generated from (III-22) .

$$X(t_{k+1}) = X_0(t_{k+1}) + X_1(t_{k+1})$$

where

$$\begin{aligned} X_i(t_{k+1}) &= \phi_{i,11}(\Delta_k)\,X_i(t_k) + \phi_{i,12}(\Delta_k)\,X_{i,2}(t_k) + \theta_{i,k} \\ X_{i,2}(t_{k+1}) &= \phi_{i,21}(\Delta_k)\,X_i(t_k) + \phi_{i,22}(\Delta_k)\,X_{i,2}(t_k) + \eta_{i,k} \end{aligned} \qquad i=0,1$$

In order for X_0 and X_1 to be independent

$$E[\theta_{0,k}\,\theta_{1,k}] = E[\eta_{0,k}\,\eta_{1,k}] = E[\theta_{0,k}\,\eta_{1,k}] = E[\eta_{0,k}\,\theta_{1,k}] = 0$$

must be satisfied and hence four sequences of random numbers must be generated instead of two sequences as before. The matrices $\phi_{0,ij}(t)$ and $\phi_{1,ij}(t)$ for this case are given by (III-17) where $w_0^2 = \lambda_0^2 - a^2$ for $\phi_{0,ij}(t)$ and $w_1^2 = \lambda_1^2 - a^2$ for $\phi_{1,ij}(t)$.

The expressions for $\theta_{i,k}$ and $\eta_{i,k}$ are taken from (III-24) and are of the form

$$\theta_{i,k} = A_{i,k} \cos \alpha_{i,k} + B_{i,k} \sin \alpha_{i,k}$$

$$\eta_{i,k} = - A_{i,k} \sin \alpha_{i,k} + B_{i,k} \cos \alpha_{i,k} \qquad i=0,1$$

where $\{A_{i,k}\}$, and $\{B_{i,k}\}$ are four sequences of independent, zero mean, unit variance Gaussian random numbers and $\alpha_{i,k}$ is defined by (III-25).

$$\alpha_{i,k} = \tan^{-1} \left[2\rho i \, \sigma_{\theta_i} \sigma_{\eta_i} / \left(\sigma_{\eta_i}^2 - \sigma_{\theta_i}^2 \right) \right]$$

The values of ρ_i, σ_{θ_i} and σ_{η_i} are obtained from (III-19) through (III-21). Specifically,

$$\sigma_{\theta_i}^2 = 1 + e^{-2a \Delta_k} \left(a \, w_i \sin 2 w_i \bar{\Delta}_k + a^2 \cos 2 w_i \Delta_k - \lambda_i^2 \right) / w_i^2$$

$$\sigma_{\eta_i}^2 = \lambda_i^2 - \lambda_i^2 e^{-2a \Delta_k} \left(a \, w_i \sin 2 w_i \Delta_k - a^2 \cos 2 w_i \Delta_k + \lambda_i^2 \right) / w_i^2$$

$$\rho_i = \left(a \lambda_i^2 e^{-2a \Delta_k} (\cos 2 w_i \Delta_k - 1) / w_i^2 \right) / \sigma_{\theta_{i,k}} \sigma_{\eta_{i,k}}$$

where

$$w_i^2 = \lambda_i^2 - a^2 \quad i=0,1 \, .$$

IV. SIMULATION RESULTS

The simulation was performed for each of the three spectral densities using the uniformly sampled periodic estimator and the Poisson estimator. For each case simulated both estimators were provided with the same or corresponding parameter values. The number of time samples was held constant and equal to 1000, and the Parzen window h(t), given by

$$h(t) = \begin{cases} 1 - 6\,t^2 + 6\,|t|^3 & |t| \leq \frac{1}{2} \\ 2\,(1 - |t|)^3 & \frac{1}{2} < |t| \leq 1, \\ 0 & 1 < |t| \end{cases} \qquad \text{(IV-1)}$$

was used as the covariance averaging kernel for both estimators. The Parzen spectral window was chosen because it reduces the variance of the estimate and is everywhere positive in the frequency domain. This spectral window eliminates the possibility of yielding negative estimates for the periodic estimator and reduces the probability of negative estimates for the Poisson estimator. Corresponding sampling rates ρ for the periodic case and (average) sampling rates for the Poisson were used for each spectral density, specifically $\rho = \beta$ for each case. Several different values of the sampling rates were considered for each spectral density in order to determine their effect on the estimates.

The value of the truncation point M_N of the estimators was chosen for each case as the value which minimizes the mean squared error over the frequency range investigated. The procedure for choosing the M_N was to compute several estimates of the same spectral density while varying M_N and then selecting the M_N for the case of smallest mean squared error. The values of M_N for the periodic and the Poisson estimators do not, in general, coincide. This is because the periodic estimator is actually estimating the aliased spectral density rather than the true spectral density as in the Poisson case.

The results of the simulation for each of the three spectral densities are presented in the following sections and a summary of this work appears in [7].

A. First Order Gauss-Markov Case

For this case three sampling rates were used for both the Poisson and periodic estimates. These are $\rho = \beta = 2, 4$ and 2π radians/second. For the Poisson case the sampling rates correspond to average values. These rates were chosen as being multiples ($2, 4, 2\pi$) of the half power point of the spectral density. They are representative of sampling at approximately the 4, 9 and 13 dB down points of the spectral density. The number of data points used in the simulation was N = 1000. M_N was selected on the basis of smallest mean square error, the Parzen spectral window (IV-2) was used and $\alpha = 1.0$.

Spectral estimates for these sampling rates are shown in Figures 4, 5, and 6. The continuous curve appearing on the graphs represents the true continuous time spectral

density $\phi(\lambda)$. The spectral estimate $\hat{\phi}(\lambda)$ for the Poisson case and $\hat{\psi}(\lambda)$ for the periodic is represented by a continuous curve with square symbols. The graphs for the periodic case also contain a dotted curve representing the aliased spectral density $\psi(\lambda)$.

Figure 4 compares the two sampling techniques for $\rho = \beta = 2$ radians/second. The periodic graph shows a large amount of aliasing with period $2\pi\rho$ which inhibits for any λ a reasonable representation of the true spectral density $\phi(\lambda)$. On the other hand the graph representing the Poisson technique does not indicate any aliasing effects and for all λ presented on the graph a fair estimate is provided.

By doubling the sampling rate to $\rho = \beta = 4$ it is seen, Figure 5, that aliasing in the periodic estimate is reduced. This is because as ρ becomes larger $\phi(\lambda)$ becomes smaller outside the interval $[-\pi\rho, \pi\rho]$. This estimate for the periodic case is still very poor. The corresponding Poisson spectral estimate is very good with only slight fluctuations from the true spectral density $\phi(\lambda)$. The reason this estimate is so good, especially at the origin ($\lambda = 0$), is that from (II-14) $\beta = 4$ rad/s is near the optimal (π rad/s) for λ on or near the origin.

The periodic spectral estimate for the sampling rate $\rho = \beta = 2\pi$ rad/s, Figure 6, begins to resemble the true spectral density $\phi(\lambda)$ but is still heavily influenced by the aliasing error. The Poisson estimate still provides a good estimate, especially in the tail $\lambda \geqslant 2$.

For curiosity's sake the frequency axis of the Poisson graphs was extended to $\lambda = 21$ and spectral estimates were computed. The resulting estimate, which is not shown here, closely followed the true spectral density all the way to $\lambda = 21$ with no sign of aliasing or increasing error.

B. Narrowband Case

Here the two estimates (II-11) and (II-13) were evaluated for the sampling rates

$$\rho = \beta = 2\pi a \cong 0.6 \text{ rad/s} \qquad \text{(IV-2a)}$$

$$\rho = \beta = 2.2 \text{ rad/s} \qquad \text{(IV-2b)}$$

$$\rho = \beta = 3.2 \text{ rad/s} \qquad \text{(IV-2c)}$$

The sampling rates were chosen to represent a sampling rate well below Nyquist (IV-2a), one at the 3 dB point on the spectral density (IV-2b) and finally a sampling rate (IV-2c) far above the center frequency. The first rate ($2\pi a$ rad/s), in addition to being below Nyquist, is well below the peak of the spectral density. From (II-14), this is the optimal rate for estimating the peak at $\lambda = \lambda_o$.

As with the first spectral density simulated, N = 1000, M_N was selected on the basis of smallest mean square error, the Parzen spectral window (IV-2) was used, and the parameters a and λ_o were chosen to be 2.1/22 and 1.0 respectively.

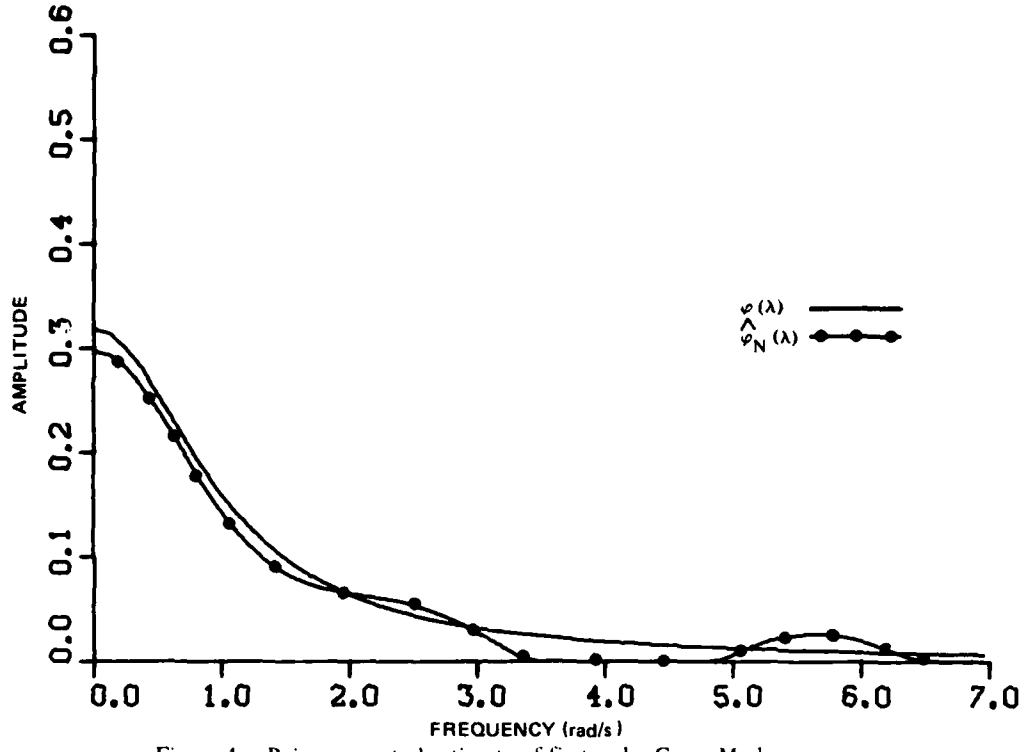

Figure 4a. Poisson spectral estimate of first order Gauss-Markov process sampled at β = 2 rad/s with M_N = 7.

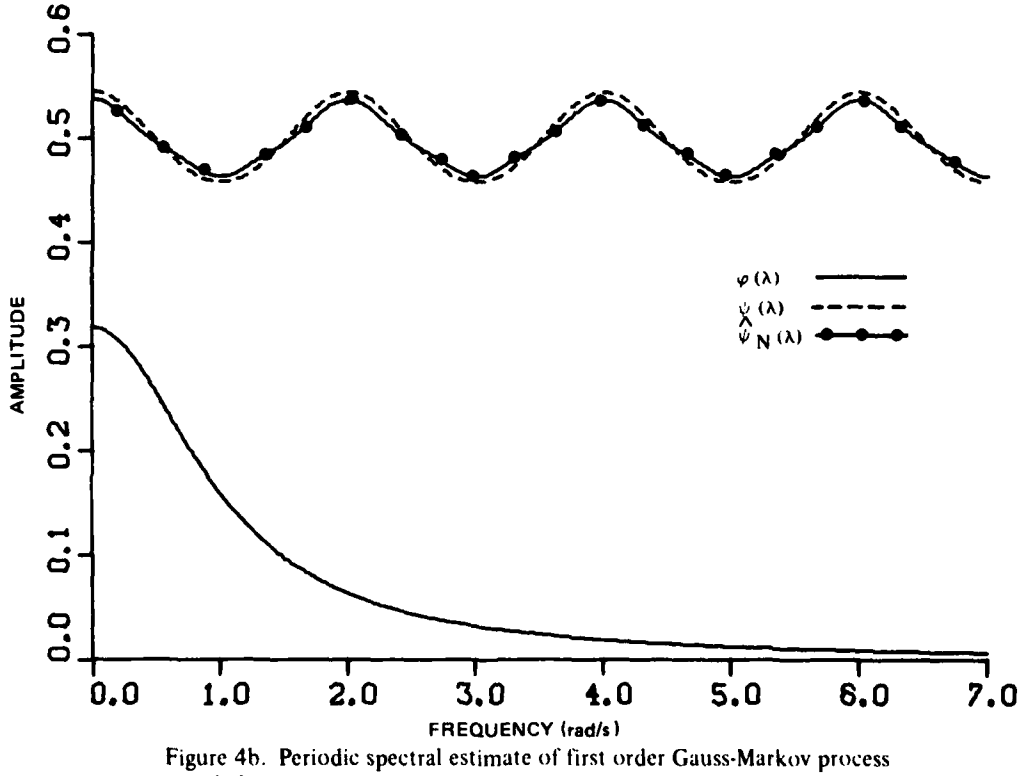

Figure 4b. Periodic spectral estimate of first order Gauss-Markov process sampled at ρ = 2 rad/s with M_N = 5.

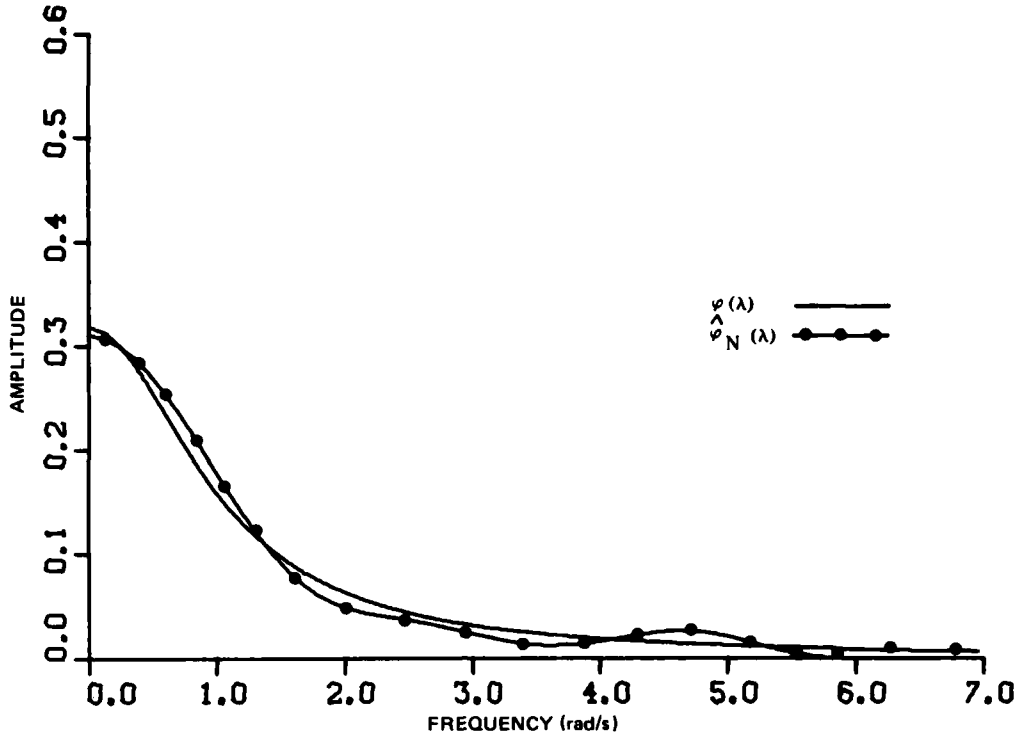

Figure 5a. Poisson spectral estimate of first order Gauss-Markov process sampled at β = 4 rad/s with M_N = 7.

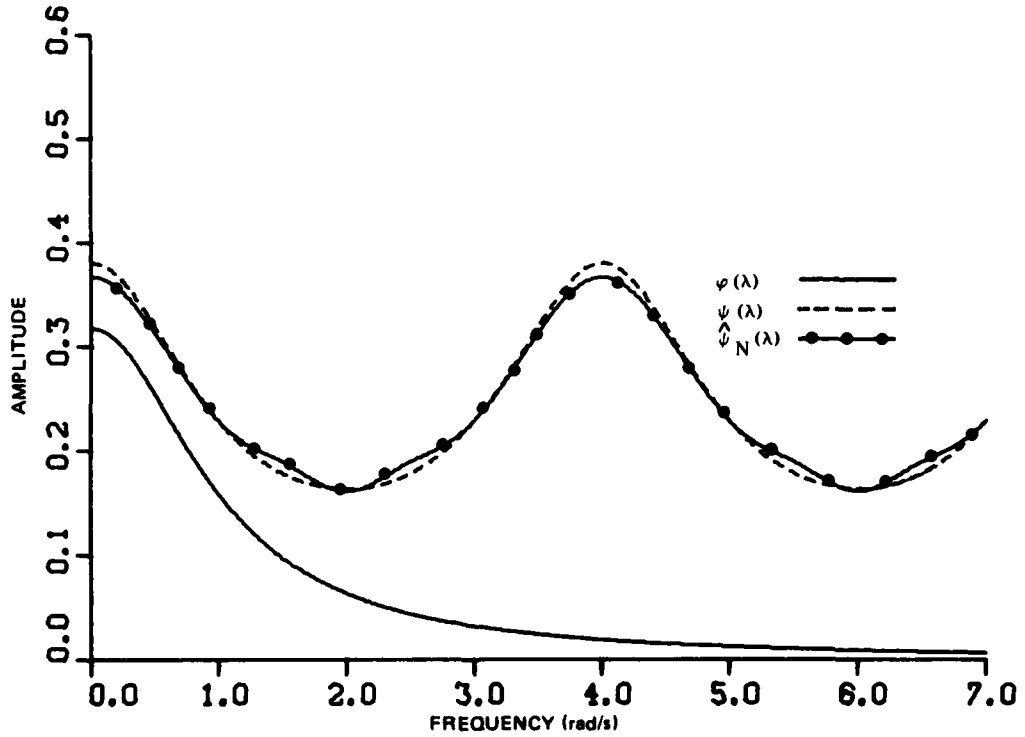

Figure 5b. Periodic spectral estimate of first order Gauss-Markov process sampled at ρ = 4 rad/s with M_N = 8.

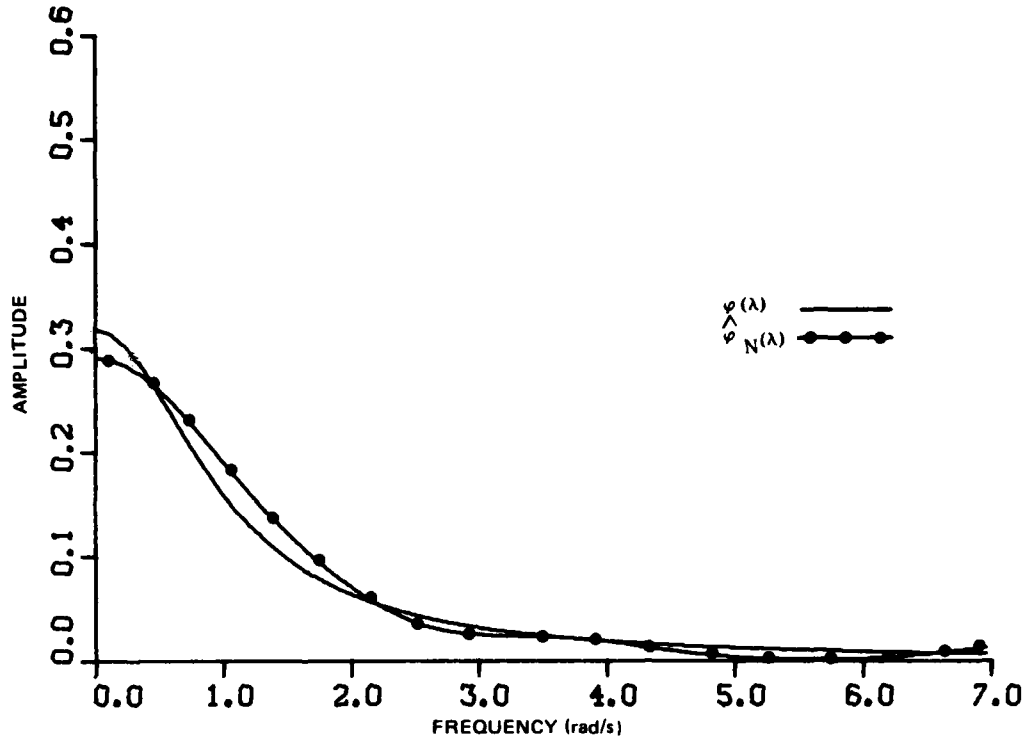

Figure 6a. Poisson spectral estimate of first order Gauss-Markov process sampled at $\beta = 2\pi$ rad/s with $M_N = 6$.

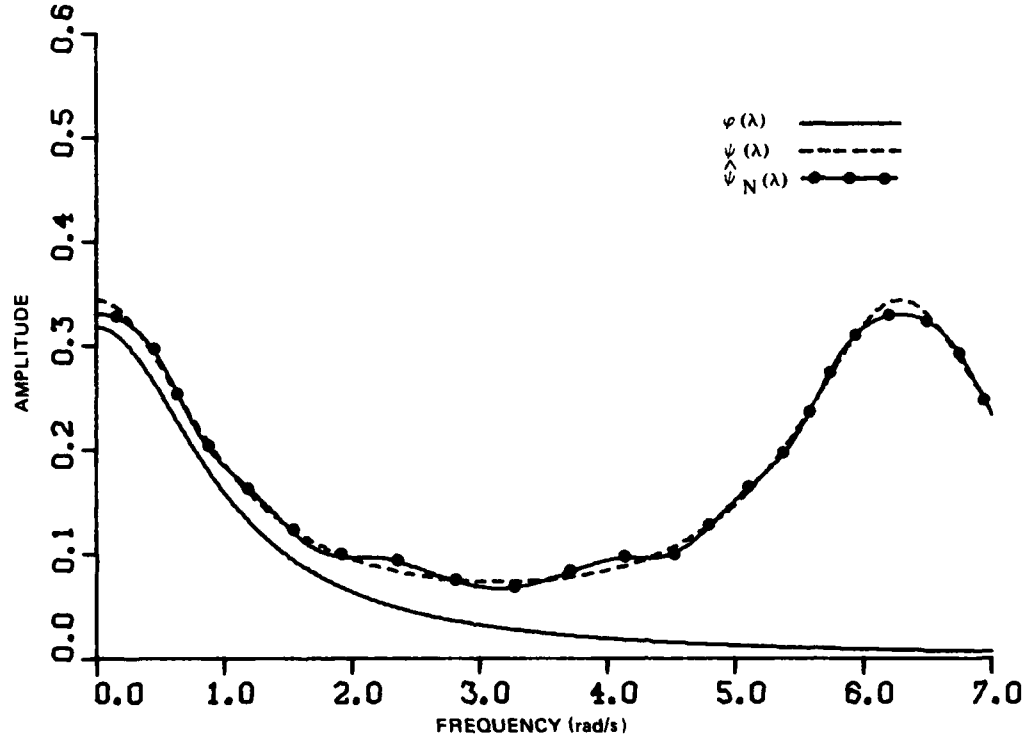

Figure 6b. Periodic spectral estimate of first order Gauss-Markov process sampled at $\rho = 2\pi$ rad/s with $M_N = 15$.

The results for the simulation of this spectral density are presented in Figures 7 through 9. Figure 7 shows the results of the estimates for $\rho = \beta = 2\pi a$ rad/s. This sampling rate is well below the band which is centered at $\lambda_0 = 1$. The periodic estimate shows no resemblance whatsoever to the true spectral density $\phi(\lambda)$. The majority of the error is due to spectral aliasing. The Poisson estimate for this case provides a slight bias, in frequency, but otherwise a very good estimate of the spectral density. No aliasing is present in this graph for any λ. Figure 8 shows the spectral estimates for the second sample rate $\rho = \beta = 2.2$ rad/s. The Poisson estimate in this case undershoots the peak at $\lambda = 1$ by about 20% which is about 1.0 dB. The periodic estimate is much improved in terms of aliasing for this sample rate but is still poor for frequencies between $\lambda = 1.0$ and $\lambda = 1.5$. The estimate is biased in amplitude for most of the λ but for portions of the spectral density the estimate is reasonable. If we had extended the frequency axis of the graphs for the periodic case another pair of peaks would erroneously appear every multiple of $2\pi\rho$. This would not occur for the Poisson estimate. The third sampling rate, $\rho = \beta = 3.2$ rad/s, was used to generate the estimates shown in Figure 9. In this case, for $\lambda < 1.5$, the periodic estimate is very good but for $\lambda > 1.5$ the aliasing error dominates. The Poisson estimate gives a good representation of the true spectral density over the entire range of the graph.

C. Two Closely Spaced Signals

This case, as described earlier, was generated by adding the time series of two narrowband signals with different center frequencies. The center frequency spacing was determined in such a way that the null between the two peaks is located at the common half power point (–3 dB) of the two peaks. The values of the parameters in equation (III-28) used for the simulation are the same as in the narrowband case with the addition of the parameter $\lambda_1 = 1.334$. Because the bandwidth (III-9) is dependent on the center frequency the bandwidth and the height of the two peaks differ slightly. Two sampling rates were used in evaluating the estimators for this spectral density:

$$\rho = \beta = 2\pi a \text{ rad/s} \qquad \text{(IV-3a)}$$

$$\rho = \beta = 3.2 \text{ rad/s.} \qquad \text{(IV-3b)}$$

These two sampling rates provide an example of sampling well below the two peaks and another of sampling above them in frequency. Other parameters used for this spectral density are identical to the narrowband case (i.e. N = 1000, a = 2.1/22). The results for this spectral density are presented in Figures 10 and 11. Figure 10 shows the results for the sample rate ($2\pi a$ rad/s). The randomly sampled estimate (top of Figure 10) shows fairly large oscillations with frequency but does succeed in providing a fair estimate of the spectral density. It is of significance that even though the crossover point between the two peaks is

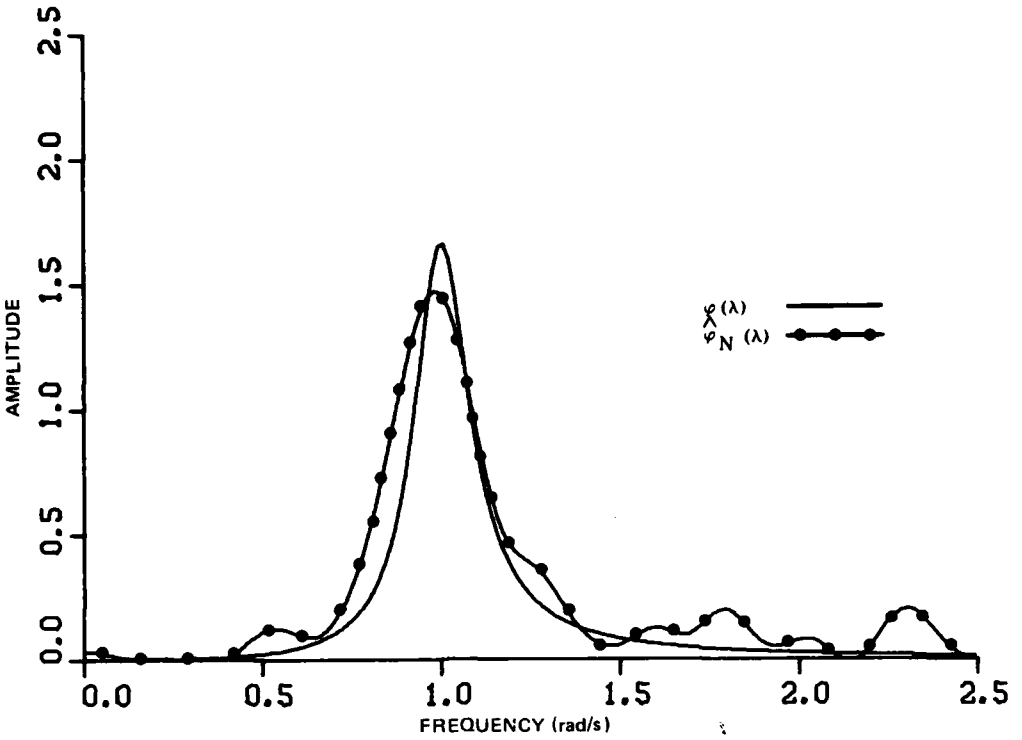

Figure 7a. Poisson spectral estimation for "narrowband" spectral density sampled at $\beta = 2\pi$ a ~0.6 rad/s, with $M_N = 50$.

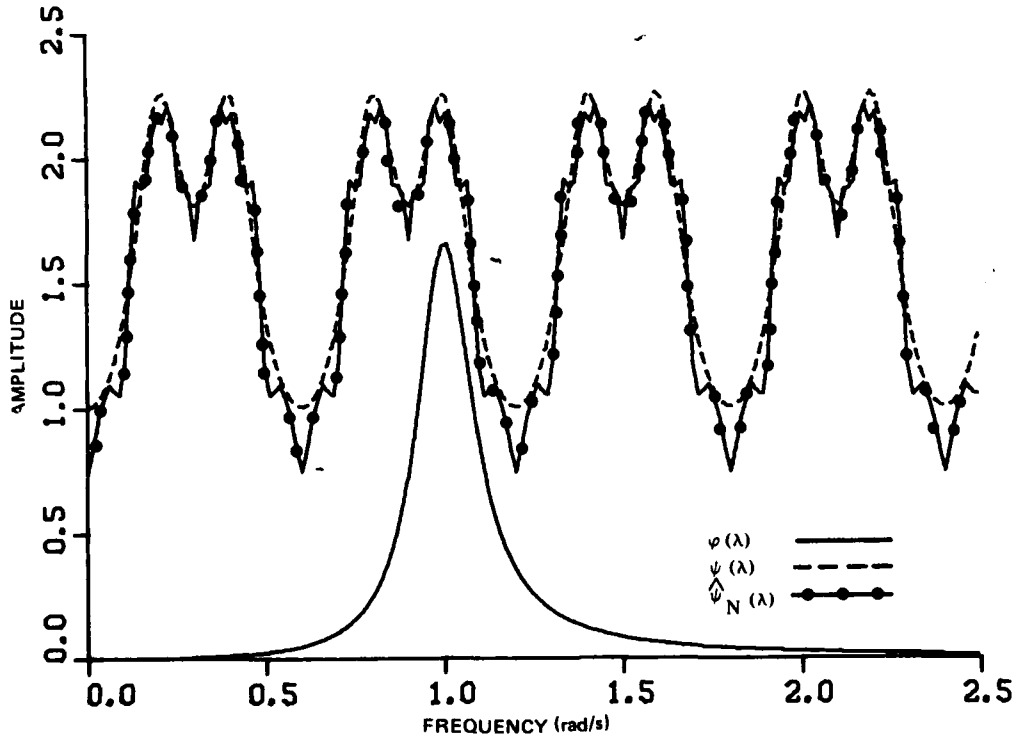

Figure 7b. Periodic spectral estimation of "narrowband" spectral density sampled at $\rho = 2\pi$ a ~0.6 rad/s with $M_N = 25$.

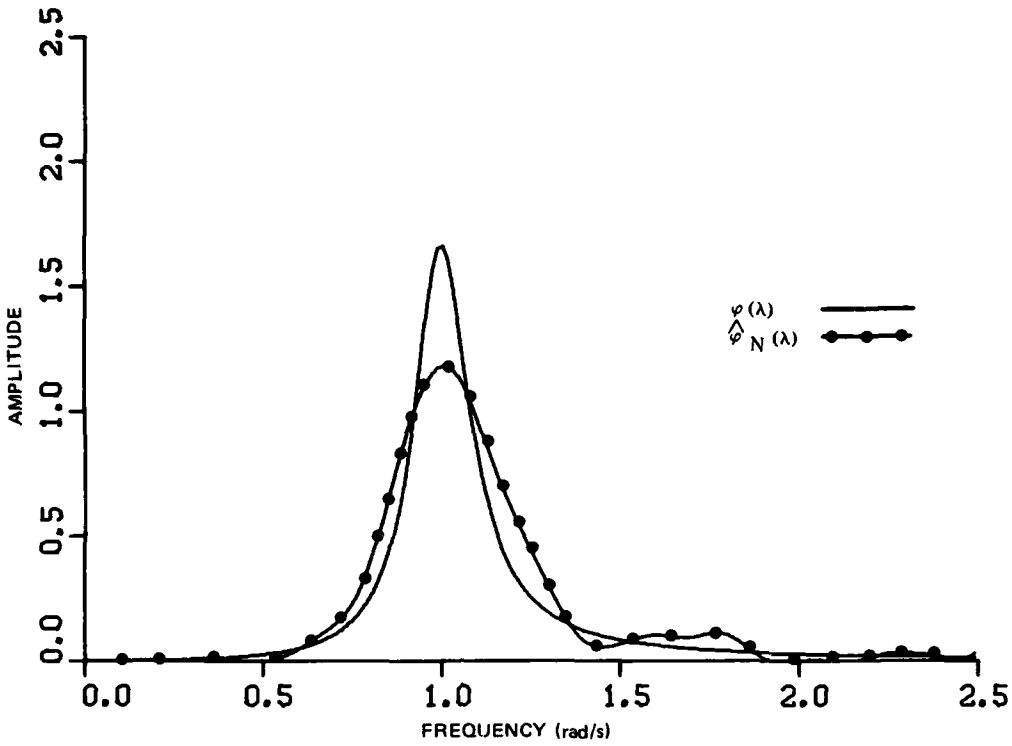

Figure 8a. Poisson spectral estimation of "narrowband" spectral density sampled at $\beta = 2.2$ rad/s with $M_N = 55$.

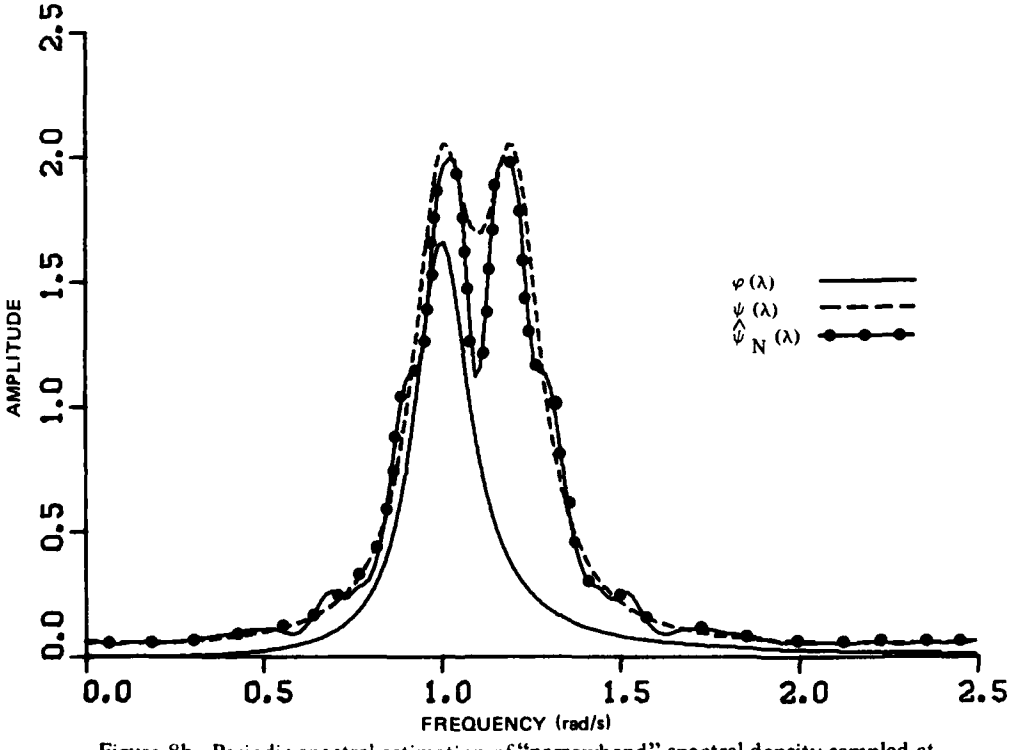

Figure 8b. Periodic spectral estimation of "narrowband" spectral density sampled at $\rho = 2.2$ rad/s with $M_N = 50$

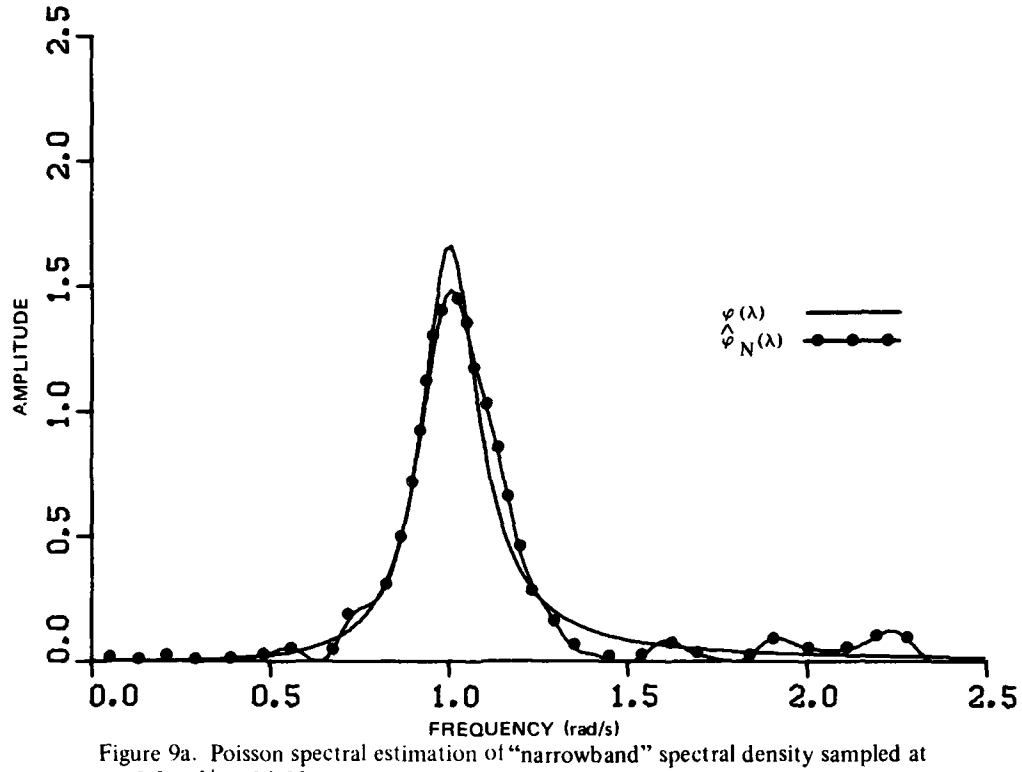

Figure 9a. Poisson spectral estimation of "narrowband" spectral density sampled at $\beta = 3.2$ rad/s, with $M_N = 70$.

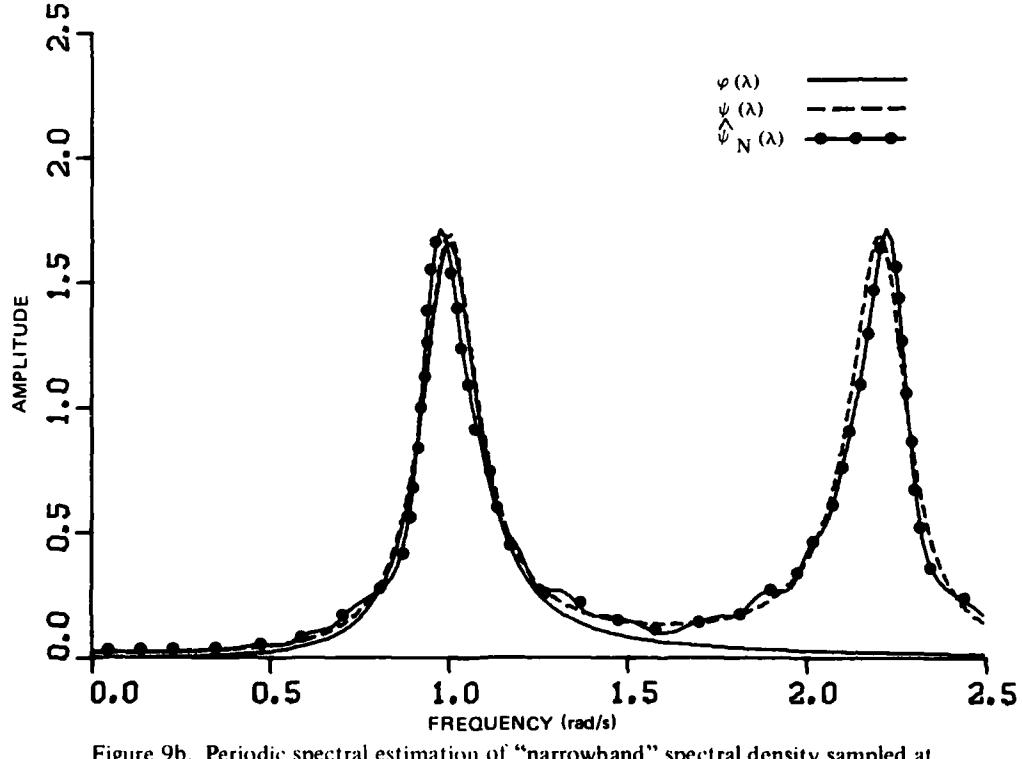

Figure 9b. Periodic spectral estimation of "narrowband" spectral density sampled at 3.2 rad/s with $M_N = 55$.

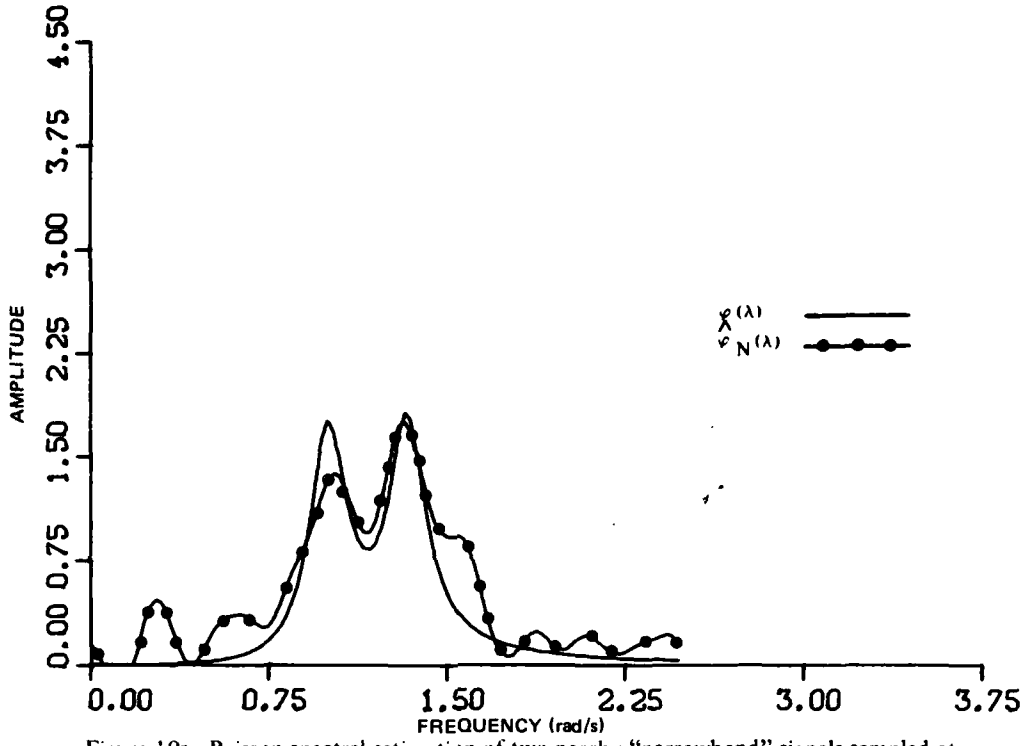

Figure 10a. Poisson spectral estimation of two nearby "narrowband" signals sampled at $\beta = 2\pi$ a ~0.6 rad/s with $M_N = 55$.

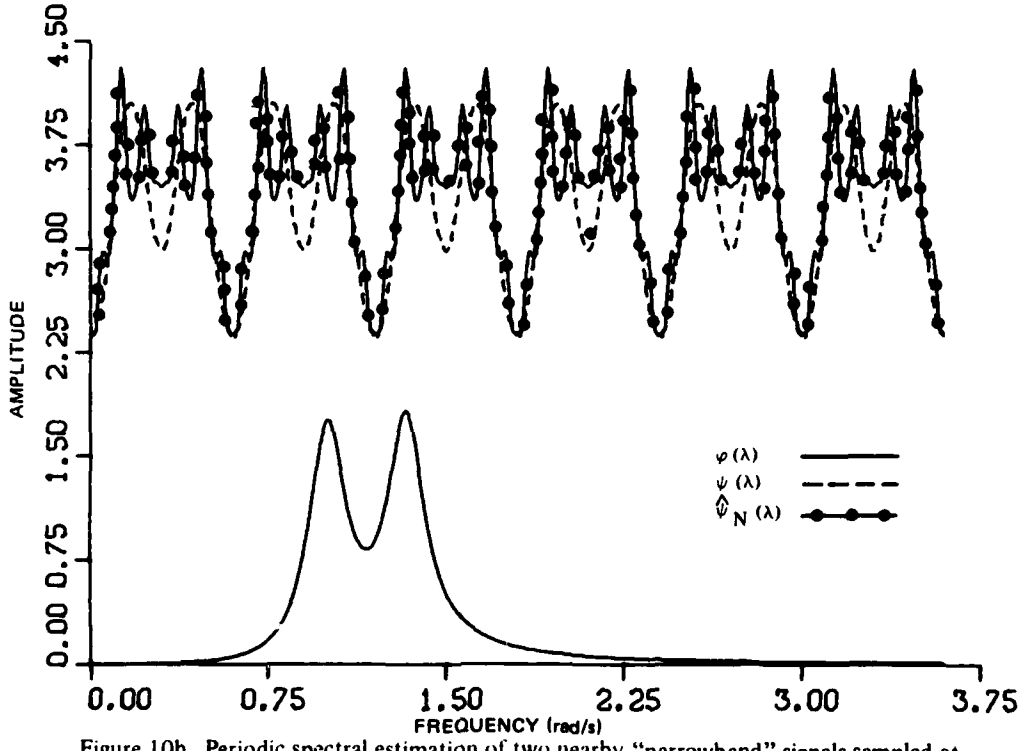

Figure 10b. Periodic spectral estimation of two nearby "narrowband" signals sampled at $\rho = 2\pi$ a ~0.6 rad/s with $M_N = 20$.

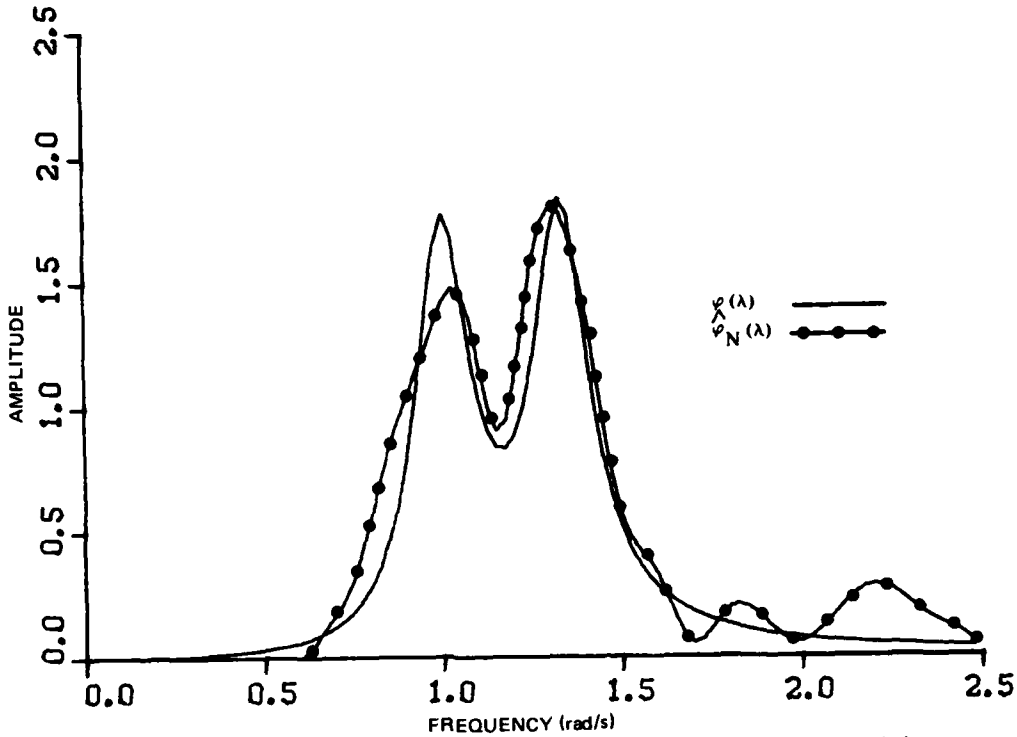

Figure 11a. Poisson spectral estimation of two nearby "narrowband signals sampled at $\beta = 3.2$ rad/s with $M_N = 60$.

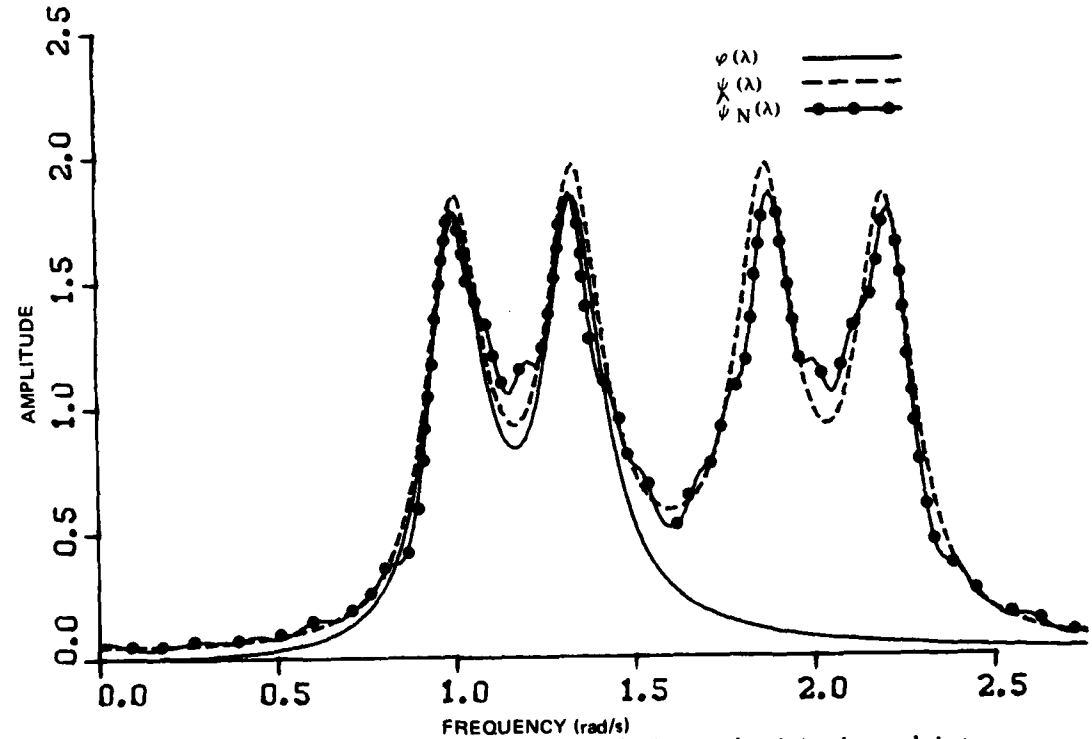

Figure 11b. Periodic spectral estimation of two nearby "narrowband signals sampled at $\rho = 3.2$ rad/s with $M_N = 55$.

only 3 dB the estimate does indeed separate the peaks. For the periodically sampled estimate there is no resemblance of the estimate to the true spectral density. In this case the aliased spectral density is not even well estimated. It should be noted that the amplitude axis has been scaled down in the graphs to accommodate the large aliasing effects from the periodic estimates. Figure 11, which is for a sample rate of 3.2 rad/s, is improved for both the random case and the periodic case. The random estimate demonstrates less variance but otherwise has changed very little. This shows, as in the other spectral densities simulated, that the Poisson technique does not depend strongly on the sampling rate. On the other hand, the periodic estimate shown in Figure 10 is much improved, particularly for $\lambda < 1.5$. Still, for the estimate at higher frequencies in Figure 11 the aliasing error drastically distorts the estimate.

D. Data Integrity

In a simulation study where synthetically generated data are used the question concerning the quality of the data arises. The theory assumes the Poisson sample spacings (III-6) and the data X(t) are uncorrelated from sample to sample. In addition, the Poisson sample spacings and the data are assumed not to be cross correlated. Unfortunately, for a simulation of this type that is not possible.

A random number generator* was used to generate exponentially distributed (mean = 1) random numbers $\{\alpha\}_{k=1}^{N}$ for the Poisson sample times $\{t_k\}_{k=1}^{N}$ and normal (0, 1) random numbers which were used as a basis for simulating the data $\{X\}_{k=1}^{N}$. Sample auto- and cross-correlations for the random numbers used in the simulation were calculated. The sample correlations resulting from random numbers used in the first order Gauss-Markov spectral density for lags to ±10 were calculated and the more significant values are given in Table 1. For the autocorrelations, normalized to 1 at zero lag, the correlations were considered acceptable with the exception of $\{\alpha_k\}$ for lag ± 1. Similarly the crosscorrelation values under 1.0% were considered good. It is possible that numbers with smaller sample correlation values could have been generated with successive computer runs, but numbers with sample correlations of this order were considered to be representative of the random number generator and therefore the results of this simulation could easily be duplicated.

Another approach would have been to generate many sets of numbers and compute spectral estimates for each set of numbers and average them together. This would have been very costly and since this simulation compares two different spectral estimation techniques, this was not necessary.

Sample correlation values for random numbers used in the other spectral densities simulated were very similar to those in Table 1 and are not presented here.

*A software random number generator from the International Mathematics and Statistics Library (IMSL) was used for the random numbers. The UNIVAC 1110 computer was used in the simulation.

TABLE 1

	$\{X_k\}$	$\{\alpha_k\}$	$\{\alpha_k\}\{X_k\}$
Minimum			
of ±10 lags	4.27×10^{-4}	2.60×10^{-4}	8.03×10^{-5}
lag = 3	2.3×10^{-3}	1.84×10^{-2}	2.61×10^{-2}
= 2	3.2×10^{-3}	2.64×10^{-4}	5.40×10^{-3}
= 1	-1.2×10^{-3}	-7.20×10^{-2}	-3.23×10^{-2}
= 0	1.0	1.0	8.03×10^{-5}
= -1	-1.2×10^{-3}	-7.20×10^{-2}	5.80×10^{-3}
= -2	3.2×10^{-3}	2.64×10^{-4}	-2.37×10^{-2}
= -3	2.3×10^{-3}	1.84×10^{-2}	4.81×10^{-3}
Maximum			
of ±10 lags	3.86×10^{-2}	-7.20×10^{-2}	5.86×10^{-2}

SAMPLE AUTO CORRELATION FOR DATA $\{X_k\}$, POISSON SAMPLE TIMES $\{\alpha_k\}$ AND SAMPLE CROSS CORRELATION FOR $\{X_k\}$ AND $\{\alpha_k\}$. AT LEFT IS CORRELATION LAG AND MINIMUM AND MAXIMUM CORRELATION OVER THE LAG RANGE ±10.

V. CONCLUSIONS

The objective of this work was to provide a fair comparison between two techniques for estimating the spectral density of a continuous time stationary process.

The main feature of the Poisson spectral estimation technique is its ability to estimate the continuous time spectral density $\phi(\lambda)$ rather than the aliased discrete spectral density $\psi(\lambda)$. It is this property that eliminates the problem of spectral aliasing which is inherent in some degree in all real world spectral analysis.

From the results presented in this paper it can be concluded that the Poisson technique out-performs the periodic technique in a wide variety of circumstances. This is significant because the periodic technique is the standard method used in spectral analysis. In the first order Gauss-Markov case the Poisson technique was shown to yield good estimates of a "wide band" low pass spectral density. The successful estimation of the more complicated "narrowband" spectral density demonstrated the Poisson technique's ability to handle spectral estimates of the "narrowband" class. Finally, in the last case considered, the Poisson technique showed the ability to distinguish two "narrowband" signals closely spaced in frequency. These three spectral densities were chosen for the simulation largely because they represent the type of spectra typically encountered in ocean data.

The comparison of the Poisson and periodic techniques for the spectral densities studied showed the Poisson to clearly excel in the following cases:

a. When the spectral density is not bandlimited.

b. When the shape of the spectral density is not known a priori.

c. When the sampling rate is constrained to be below that of Nyquist.

If the signal to noise ratio and noise power are known beforehand the optimal sampling rate for them may be computed and the Poisson technique used to provide spectral estimates

The main disadvantage of the Poisson technique is that it is more difficult to implement than the periodic technique since FFT (fast Fourier transform) type procedures cannot be used. Development of techniques to efficiently extract Poisson distributed data samples from continuous time data and compactly perform the spectral estimates would make the Poisson technique more appealing for practical applications.

The Poisson theory applies to other areas of signal processing as well as spectral density estimation. This could result in using the Poisson technique in applications such as cross spectral estimation, estimation of the coherence function, and antenna array beamforming.

REFERENCES

1. E Masry, "Poisson sampling and spectral estimation of continuous-time process," IEEE Trans Information Theory, to appear
2. E Masry and MC Lui, "Discrete-Time Spectral Estimation of Continuous Parameter Processes – A new Consistent Estimate," IEEE Trans Information Theory, vol IT-22, May 1976
3. FJ Beutler, "Alias free randomly timed sampling of stochastic processes," IEEE Trans Information Theory, vol IT-16, p 147–152, 1970
4. HS Shapiro and RA Silverman, "Alias free sampling of random noise," J Soc Indust Appl Math, vol 8, p 225-248, 1960
5. DR Brillinger, "The spectral analysis of stationary interval functions," Proc Sixth Berkeley Symp Prob Statist, p 483–513, 1972
6. E Parzen, Times Series Analysis Papers, San Francisco: Holden-day, 1967, p 24–97
7. E Masry, D Klamer and C Mirabile, "Spectral Estimation of Continuous Time Processes: Performance Comparison Between Periodic and Poisson Sampling Schemes," IEEE Trans Automatic Control, to appear

APPENDIX

In general, if X has a rational spectral density function, i.e.

$$\phi(\lambda) = \left|\frac{P(i\lambda)}{Q(i\lambda)}\right|^2 \qquad \text{(A-1)}$$

where

a) $P(\lambda) = \sum_{j=0}^{m} b_j (i\lambda)^j$

b) $Q(\lambda) = \sum_{j=0}^{n} a_j (i\lambda)^j$

and $a_n = 1$, with $m < n$, then $X(t)$ formally satisfies the following stochastic differential equation:

$$X^{(n)}(t) + a_{n-1} X^{(n-1)}(t) + \ldots + a_o X(t) = b_m U^{(m)}(t) + \ldots + b_o U(t). \qquad \text{(A-2)}$$

$U(t)$ is a stationary white noise process with $E\, U(t)\, U^*(s) = \delta(t-s)$.

Now, (A-1) can be represented as

$$\dot{\underset{\sim}{X}}(t) = F\, \underset{\sim}{X}(t) + G\, U(t)$$

where

$$F = \begin{bmatrix} -a_{n-1} & 1 & & 0 \\ -a_{n-2} & 0 & \ddots & \\ \vdots & & & 1 \\ -a_0 & 0 & \cdots & 0 \end{bmatrix}, \qquad \text{(A-3)}$$

$$G = \begin{bmatrix} b_{n-1} \\ b_{n-2} \\ \vdots \\ b_0 \end{bmatrix},$$

$$\underset{\sim}{X}(t) = \begin{bmatrix} X_1(t) \\ X_2(t) \\ \cdot \\ \cdot \\ \cdot \\ \\ \\ \\ X_n(t) \end{bmatrix}$$

with

$$X_1(t) = X(t)$$

$$X_2(t) = \dot{X}_1(t) + a_{n-1} X(t) - b_{n-1} U(t)$$

$$\cdot$$

$$\cdot$$

$$\cdot$$

$$X_n(t) = \dot{X}_n(t) + a_1 X(t) - b_1 U(t) \ .$$

The solution of (A-1) is given by

$$\underset{\sim}{X}(t) = \Phi(t, t_o)\, \underset{\sim}{X}(t_o) + \int_{t_o}^{t} \Phi(t,\tau)\, G(\tau)\, U(\tau)\, d\tau \qquad \text{(A-4)}$$

where the state transition matrix $\Phi(t,t_o)$ satisfies the (deterministic) differential equation

$$\frac{d}{dt}\Phi(t,\tau) = F\,\Phi(t,\tau)$$

whose solution is given by

$$\Phi(t,\tau) = e^{F(t-\tau)} \qquad \text{(A-5)}$$

Equation (A-4) is known as the dynamic representation of the random process X.